

# 1 DNA methylome combined with chromosome cluster-oriented analysis

## 2 provides an early signature for cutaneous melanoma aggressiveness.

3 Arnaud Carrier<sup>1</sup>, Cécile Desjobert<sup>1</sup>, Loïc Ponger<sup>2</sup>, Laurence Lamant<sup>3</sup>, Matias Bustos<sup>4</sup>, Jorge  
4 Torres-Ferreira<sup>5,6</sup>, Rui Henrique<sup>5,6,7</sup>, Carmen Jeronimo<sup>5,6,7</sup>, Luisa Lanfrancone<sup>8</sup>, Audrey  
5 Delmas<sup>3</sup>, Gilles Favre<sup>3</sup>, Antoine Daunay<sup>9</sup>, Florence Busato<sup>10</sup>, Dave S.B. Hoon<sup>4</sup>, Jörg Tost<sup>10</sup>,  
6 Chantal Etievant<sup>1</sup>, Joëlle Riond<sup>1,3</sup>, Paola B. Arimondo<sup>1,11\*</sup>

7  
8 1-Unité de Service et de Recherche USR n°3388 CNRS-Pierre Fabre, Epigenetic Targeting of  
9 Cancer (ETaC), Toulouse, France

10 2-CNRS UMR 7196 / INSERM U1154/Sorbone university- National museum of natural  
11 history (NMNH), Paris, France

12 3-UMR 1037 INSERM/Université Toulouse III Paul Sabatier, Cancer Research Center of  
13 Toulouse, (CRCT), Toulouse, France

14 4-Department of Translational Molecular Medicine, Saint John's Cancer Institute, Providence  
15 Saint John's Health Center, Santa Monica, CA USA

16 5-Cancer Biology & Epigenetics Group, Research Center (CI-IPOP)/P.CCC Porto  
17 Comprehensive Cancer Center, Portuguese Oncology Institute of Porto (IPO Porto), Porto,  
18 Portugal

19 6-Department of Pathology, Portuguese Oncology Institute of Porto (IPO Porto)/P.CCC Porto  
20 Comprehensive Cancer Center, Porto, Portugal

21 7-Department of Pathology and Molecular Immunology, Biomedical Sciences Institute  
22 (ICBAS), University of Porto, Porto, Portugal

23 8-Instituto Europeo di Oncologia, Department of Experimental Oncology, Via Adamello 16,  
24 20139 Milan, Italy

25 9-Laboratory for Functional Genomics, Fondation Jean Dausset - CEPH, Paris, France

26 10-Laboratory for Epigenetics and Environment, Centre National de Recherche en  
27 Génomique Humaine, CEA-Institut de Biologie François Jacob, Evry, France

28 11-EpiCBio, Epigenetic Chemical Biology, Department Structural Biology and Chemistry,  
29 Institut Pasteur, CNRS UMR n°3523 Chem4Life, 28 rue du Dr Roux, 75015 Paris, France

30

31 \* Correspondence should be addressed to Dr. Paola B. Arimondo, EpiCBio Institut Pasteur –  
32 CNRS UMR3523, tel. +33 1 86 46 78 69 email: [paola.arimondo@cnrs.fr](mailto:paola.arimondo@cnrs.fr)

33

34 **Running title:** Chromosome clusters of DNA methylation mark aggressive melanoma

35 .

36

37

## 38 ABSTRACT

39 Aberrant DNA methylation is a well-known feature of tumours and has been associated with  
40 metastatic melanoma. However, since melanoma cells are highly heterogeneous, it has been  
41 challenging to use affected genes to predict tumour aggressiveness, metastatic evolution, and  
42 patients' outcomes. We hypothesized that common aggressive hypermethylation signatures  
43 should emerge early in tumorigenesis and should be shared in aggressive cells, independent of  
44 the physiological context under which this trait arises.

45 We compared paired melanoma cell lines with the following properties: (i) each pair  
46 comprises one aggressive counterpart and its parental cell line, and (ii) the aggressive cell  
47 lines were each obtained from different host and their environment (human, rat, and mouse),  
48 though starting from the same parent cell line. Next, we developed a multi-step genomic  
49 pipeline that combines the DNA methylome profile with a chromosome cluster-oriented  
50 analysis.

51 A total of 229 differentially hypermethylated genes were commonly found in the aggressive  
52 cell lines. Genome localization analysis revealed hypermethylation peaks and clusters,  
53 identifying eight hypermethylated gene promoters for validation in tissues from melanoma  
54 patients.

55 Five CpG identified in primary melanoma tissues were transformed into a DNA methylation  
56 score that can predict survival (Log-rank test,  $p=0.0008$ ). This strategy is potentially  
57 universally applicable to other diseases involving DNA methylation alterations.

## 58 Keywords

59 Epigenomics, DNA methylation, chromosome clusters, melanoma, patient outcome, genome  
60 localization, oriented-approach.

## 62 INTRODUCTION

63 Cutaneous metastatic melanoma is the deadliest form of skin cancer and its occurrence is  
64 growing (1). The recent development of targeted and immune therapies has dramatically  
65 improved patient's outcomes. Indeed, median overall survival of patients with advanced-stage  
66 melanoma has increased from ~ 9 months to at least 2 years since 2011 (2). Overall survival is  
67 better after targeted (3) or immuno therapies (4), but there are still non-responders and

neo/acquired resistants. Despite these advances, there is place for improvement in particular to discover novel early prognostic markers and potential avenue for adjuvant therapies. DNA methylation in malignant melanoma has been studied to identify specific DNA methylation changes and decipher their impact. Melanoma has a CpG island methylator phenotype (CIMP) (5), and several methylated genes are associated with melanoma progression (6), with aggressive clinical and pathological features and poor survival in patients (7,8), are candidate epigenetic drivers of melanoma metastasis (9) or are implicated in immunotherapy resistance (10). Such DNA methylation changes have been studied at different stages of the metastatic disease, but not in primary cutaneous tumour. Importantly, DNA methylation has been shown to occur very early in tumour formation (11), and thus has the potential to provide early biomarkers indicating the metastatic potential of the tumour. However, the field currently lacks a genomic strategy that can both account for genetic environment and identify early DNA methylation markers that predict the aggressiveness of melanoma.

Here, we developed a strategy that leverages the DNA methylome from different pairs of human melanoma cells lines. Cells within pairs share a common genetic background, but one counterpart has been selected for aggressiveness in different *in vivo* contexts (human *vs* murine). We proposed that the DNA methylation signature of tumour aggressiveness would be independent of the physiological context: starting from a human tumour, shared signatures relevant to aggressiveness should emerge independent on whether this trait were acquired in humans, or whether cells have been implanted into rats or mice. In a multi-step selection process, we identified hypermethylated sites common to the most aggressive melanoma forms, analysed the distribution of these sites in the genome, and validated these methylation peaks in cell lines and patient samples. This strategy identified a DNA methylation signature of five CpG sites in four gene promoters in primary tumours that could predict the overall survival of the patients and thus has potential diagnostic application. This strategy, which overcomes heterogeneity in tumours due to the environment, can potentially be generalized to other cancers involving DNA methylation alterations.

## **MATERIAL AND METHODS**

### **Cell Culture**

The WM115 and WM266-4 cell lines were obtained from the American Type Culture Collection. The WM-115 cell line was derived from a human primary melanoma in early

stages of the vertical growth phase (VGP). The WM266-4 cell line was derived from a cutaneous metastatic melanoma tumour of the same patient. The WM983A and WM983B cell lines were obtained from the Coriell Institute (USA). The WM983A was derived from a human primary melanoma in VGP and the WM983B is the cutaneous lymph node metastasis from the same patient. The M4Be cell line was established from a human cutaneous lymph node metastasis (12). The TW12 cell line is an aggressive variant of the parental M4Be cell line that was obtained *in vivo* after two serial transplantations (subcutaneous xenografts in new-born immuno-deprived rats). A subclone (TW12) was selected after limiting dilution for its high ability to form lung metastasis (13–15). The M4BeS2 cell line was obtained in the L. Lamant's laboratory according to the *in vivo* selection scheme described by Clark et al. (16). Briefly, M4Be cells were xenografted intravenously in nude mice. Lung metastases were collected, grown briefly *in vitro* and used for a second cycle of intravenous injection. Lung metastases were collected and established *in vitro* as the M4BeS2 cell line. WM983A and WM983B cell lines were grown in 20% Leibovitz L-15 medium (v/v), 2% FBS heat inactivated (v/v), 5 µg/mL insulin and 1.68 mM CaCl<sub>2</sub>. All other cell lines were grown in DMEM (Invitrogen, France) supplemented with 10% foetal bovine serum (Sigma, France), 2 mM glutamine, 100 UI/mL penicillin-streptomycin and 1.25 µg/mL fungizone (Invitrogen) in 5% CO<sub>2</sub>. Quantitation of viable cells was performed using an Automated Cell Viability Analyzer (Beckman Coulter Vi-Cell). All cell lines were stored in ampoules in liquid nitrogen after receipt. All cell lines were regularly verified for mycoplasma contamination using the MycoAlert™ Mycoplasma Detection Kit (Lonza, Switzerland) and kept for a limited number of passages in culture.

## **Tumour samples**

Tumour samples from melanoma patients were obtained from the tumour tissue bank at the Department of Pathology, IUCT-O Toulouse Hospital (France). The study was carried out in accordance with the institutional review board-approved protocols (CRB, AC-2013-1955) and the procedures followed were in accordance with the Helsinki Declaration. Pathological specimens consisted of primary melanomas ( $n = 12$ ), lymph node metastases ( $n = 7$ ), and cutaneous metastases ( $n = 3$ ). Additional primary melanoma ( $n = 5$ ) frozen samples were provided by the Department of Experimental Oncology, European Institute of Oncology, Milan (Italy). The Saint John' Cancer Institute (formerly John Wayne Cancer institute (USA)) Formalin-fixed paraffin-embedded (FFPE) specimen cohort included tissues including primary melanomas ( $n = 12$ ). A total of 20 FFPE tissues samples from patients diagnosed with

cutaneous melanoma between 2007 and 2017 at the Portuguese Oncology Institute of Porto (IPO-Porto) without any neoadjuvant treatment were included in this study. All samples were archived at the Department of Pathology of IPO-Porto. All cases were reviewed by an experienced pathologist and staged according to the 8<sup>th</sup> edition American Joint Committee on Cancer (AJCC) system (17). Relevant clinical data was collected from medical charts. For DNA extraction, a 4 µm section was cut from a representative tissue block and stained with hematoxylin-eosin. Tumour areas containing >70% transformed cells were delimited, enabling macrodissection in eight consecutive 8µm sections. This study was approved by the institutional ethics committee of IPO Porto (CES-IPOP-FG13/2016). Anonymized clinical information for all the melanoma patients analysed is available, and the clinical pathological features of primary melanoma patients are indicated below (Table1).

**Table 1.** Clinical pathological features of primary melanoma patients

<b>Variables</b>	<b>n (%)</b>
<b>Mean age (sd)</b>	66.40 (15.88)
<b>Gender</b>	
Male	26 (53)
Female	23 (47)
<b>AJCC 8<sup>th</sup> stages</b>	
IV	12 (24)
III	12 (24)
IIIA	1 (2)
IIIB	2 (4)
IIIC	2 (4)
II	2 (4)
IIA	3 (6)
IIB	6 (12)
IIC	6 (12)
IB	2 (4)
unknown	1 (2)
<b>Mutations</b>	
<i>NRAS</i>	1 (2)
<i>BRAF</i>	6 (12)
unknown	42 (86)

#### **Genomic DNA isolation**

Genomic DNA from cell lines was performed using the DNeasy Tissue kit (Qiagen, France).

Genomic DNA from frozen patient samples was isolated using the QiaAmp kit (Qiagen, France). DNA extraction from FFPE sections was performed using the FFPE RNA/DNA Purification Plus Kit (Norgen Biotek, Thorold, Canada) in accordance with manufacturer's instructions. DNA concentration and purity were determined using the NanoDrop Lite spectrophotometer (NanoDrop Technologies, Wilmington, DE, USA).

# **Illumina methylation 450K microarray analysis**

Genome-wide DNA methylation analysis was performed on three independent samples from each cell line. One microgram of DNA was bisulfite-treated using the EpiTect 96 Bisulfite Kit (Qiagen GmbH, Germany). 200 ng of bisulfite-treated DNA was analysed using Infinium HumanMethylation 450K BeadChips (Illumina Inc., CA, USA). The array allows the interrogation of more than 485,000 methylation CpG sites per sample covering 99% of RefSeq genes, with an average of 17 CpG sites per gene region distributed across the promoter, 5'-UTR, first exon, gene body, and 3'-UTR.

The samples were processed according to the manufacturer's protocol at the genotyping facility of the Centre National de Génotypage (Evry, France) without any modification to the protocol. We used the GenomeStudio® software (version 2011.1; Illumina Inc.) for the extraction of DNA methylation signals from scanned arrays (methylation module version 1.9.0, Illumina Inc.). Methylation data were extracted as raw signals with no background subtraction or data normalization. The obtained 'β' values – that is, the methylation scores for each CpG range from 0 (unmethylated, U) to 1 (fully methylated, M) on a continuous scale – were calculated from the intensity of the M and U alleles as the ratio of fluorescent signals ( $\beta = (\text{Max}(M,0)) / (\text{Max}(M,0) + \text{Max}(U,0) + 100)$ ).

All pre-processing, correction and normalization steps were performed using an improved version of the in-house developed pipeline using subset quantile normalization based on the relation to sequence annotation provided by Illumina (18). Probes were considered as differentially methylated if the absolute value of the difference between robust median β-values in samples of each phenotypes was higher than 0.2: median cell line 1 ( $\beta_1, \beta_2, \beta_3$ ) – median cell line 2 ( $\beta_1, \beta_2, \beta_3$ )  $\geq 0.2$ , where  $\beta_1, \beta_2$ , and  $\beta_3$  corresponds to the β-values in three replicates within each cell line, all with a detection p-value < 0.01. This 0.2 threshold, representing approximately a difference in DNA methylation levels of 20%, corresponds to the recommended differences between samples analysed with the Illumina methylation Infinium technology that can be detected with a 99% confidence.

Differential DNA methylation markers were identified using a combination of two approaches. The performance of individual CpGs was assessed testing the absolute DNA methylation difference between samples of the two phenotypes of interest with different thresholds and permitting a small number of misclassifications. At the same time a vector quantization method (nearest centroid classifier) was used to define CpGs that separate, at a given threshold, the two phenotypes of interest. CpGs that were significant in both tests, were used to calculate a vector using a directed z-score, which was subsequently used to assign new samples to their phenotypic group.

The corresponding genes were obtained from a list of differentially methylated probes using the Illumina annotation file and overlap between gene lists from the three cellular pairs was determined.

The promoter methylation scores (%) reported in Figure S1 were defined as follows: mean (probe1  $\beta$ -value to probe n  $\beta$ -value)  $\times 100$ , where probe 1 to probe n are probes that are differentially methylated between WM266 vs WM115 cells (with a difference threshold 0.2 on a scale from 0 to 1) and located in the promoter region (TSS1500-TSS200-5'UTR-1<sup>st</sup> exon).

## **Bisulfite pyrosequencing**

Quantitative DNA methylation analysis was performed by pyrosequencing of bisulfite-treated DNA as described in Tost and Gut, 2007 (19). CpGs for validation were amplified using 20 ng of bisulfite treated human genomic DNA and 5–7.5 pmol of forward and reverse primer, one of them being biotinylated. Oligonucleotide sequences for PCR amplification and pyrosequencing are given in the supplementary data (Supplementary Dataset2). Reaction conditions were 1  $\times$  HotStar® Taq buffer (Qiagen) supplemented with 1.6 mM MgCl<sub>2</sub>, 100  $\mu$ M dNTPs and 2.0 U HotStar Taq polymerase (Qiagen) in a 25  $\mu$ L volume. The PCR program consisted of a denaturing step of 15 min at 95°C, followed by 50 cycles of 30 s at 95°C, 30 s at the respective annealing temperature and 20 s at 72°C, with a final extension of 5 min at 72°C. A total of 10  $\mu$ L of PCR product was rendered single-stranded as previously described and 4 pmol of the respective sequencing primers were used for analysis. Quantitative DNA methylation analysis was carried out on a PSQ 96MD system with the PyroGold SQA Reagent Kit (Qiagen) and results were analysed using the PyroMark software (V.1.0, Qiagen).

Percentages of methylation (%CpG) were measured for each individual CpG present in the regions analysed by pyrosequencing. The regions chosen were around the CpGs identified by



the Illumina methylation 450K analysis and include other CpGs. DNA methylation heatmaps were obtained using Prism8® software. The heatmaps in Figure 3 refer to the median of the median of the methylation percentages of the *n* CpG analysed by pyrosequencing (median (CpG1:%,...CpGn:%)). For each analysed gene, the difference of methylation percentages of gene promoter regions comparing WM266-4 and WM155, reported in Supplementary Figure 2A, was calculated as follows: median [(CpG1:%,...CpGn:%) in WM266-4 cells] - median [(CpG1:%,...CpGn:%) in WM115 cells].

## Definition of the signature score

The signature score considered the individual methylation values (percentages) of the selected single CpGs associated with *MYH1*, *PCDHB16*, *PCDHB15*, and the mean methylation values for the two CpGs selected for *BCL2L10*. For each gene, these methylation values were compared to the methylation median calculated from all the primary samples. A score of 1 was attributed to the gene when the methylation values differed by at least 15%. For *MYH1*, for which hypomethylation was associated with aggressiveness, this score was attributed when the methylation value was inferior to the median. Conversely, a score of 1 indicated a methylation value superior to the median for the three other genes (*PCDHB16*, *PCDHB15* and *BCL2L10*). The signature score was the sum of the scores attributed individually to the 4 genes and fell between 0 and 4. Signature score and survival information were reported in Supplementary Dataset3. This score was evaluated for each gene to assess potential correlation between individual gene scores. A random simulation using R software and based on a Chi-square test indicate that the methylation of these genes was independent from one another  $p < 0.01$ . Kaplan-Meier plots were created using GraphPad Prism8 software. The survival in months was indicated depending whether the score was under versus equal or superior than 2. Survival analysis was performed using a log-Rank and the Gehan-Breslow-Wilcoxon test with a  $p$ -value  $< 0.001$  for each considered significant. Hazard ratio was estimated on R software using survival, survminer and ggplot2 packages.

## Methylation cluster identification through statistical analysis of the distribution of the hypermethylated genes

Identified methylation clusters highlight regions where the methylation distribution on the chromosome is not random. Maps of the 229 hypermethylated genes were visualized on the Ensembl website using the tool view on karyotype (<http://www.ensembl.org>). Sex chromosomes were excluded from the analysis. The clusters were defined as a group of at



least two methylated genes in close proximity separated by non-methylated genes. The statistical relevance of the number of observed clusters on each chromosome was addressed using bootstrapping. For each simulation, methylated and non-methylated genes were randomly repositioned (shuffled) along each chromosome before recomputing the number of clusters. One thousand simulations were performed to estimate the probability of obtaining the number of observed clusters. All analyses were performed using custom-written scripts implemented in the statistical programming language R (<http://cran.r-project.org/>). All R-scripts are available from the authors upon request.

## Functional annotation and pathway analysis

The list of hypermethylated genes was imported into QIAGEN's Ingenuity® Pathway Analysis (IPA®, QIAGEN Redwood City, [www.qiagen.com/ingenuity](http://www.qiagen.com/ingenuity)). In IPA hypermethylated genes were mapped to molecular and cellular functions and to networks available in the ingenuity database and then ranked by score or p-value ( $p < 0.05$ ).

## RESULTS

### **A three-step strategy identifies differentially methylated genes that identify melanoma aggressiveness.**

To identify genes whose DNA methylation state is related to the metastatic melanoma aggressiveness; we designed a strategy to compare the DNA methylome of three pairs of melanoma cell lines. Each pair was derived from the same patient melanoma cell lines that differed in aggressiveness and microenvironmental exposure with respect to their clinical origin or subsequent *in vivo* experimental processing (Figure 1). The first pair consisted of the WM115 and WM266-4 cell lines, derived from a vertical growth phase (VGP) primary melanoma and a cutaneous metastasis from the same patient, respectively, thus comparing a less and more aggressive pair of human melanoma cells. The second and the third pairs include a cell line established from a human lymph node metastasis (M4Be) and two metastatic variants selected for their increased metastatic potential in xenograft experiments either in mouse (M4BeS2) or in rat (TW12), (Figure 1A, step 1). It is important to note that in each pair, the aggressive cell line is derived from the same genetic background, but the most aggressive lines emerged in different *in vivo* contexts: human, mouse and rat, respectively.

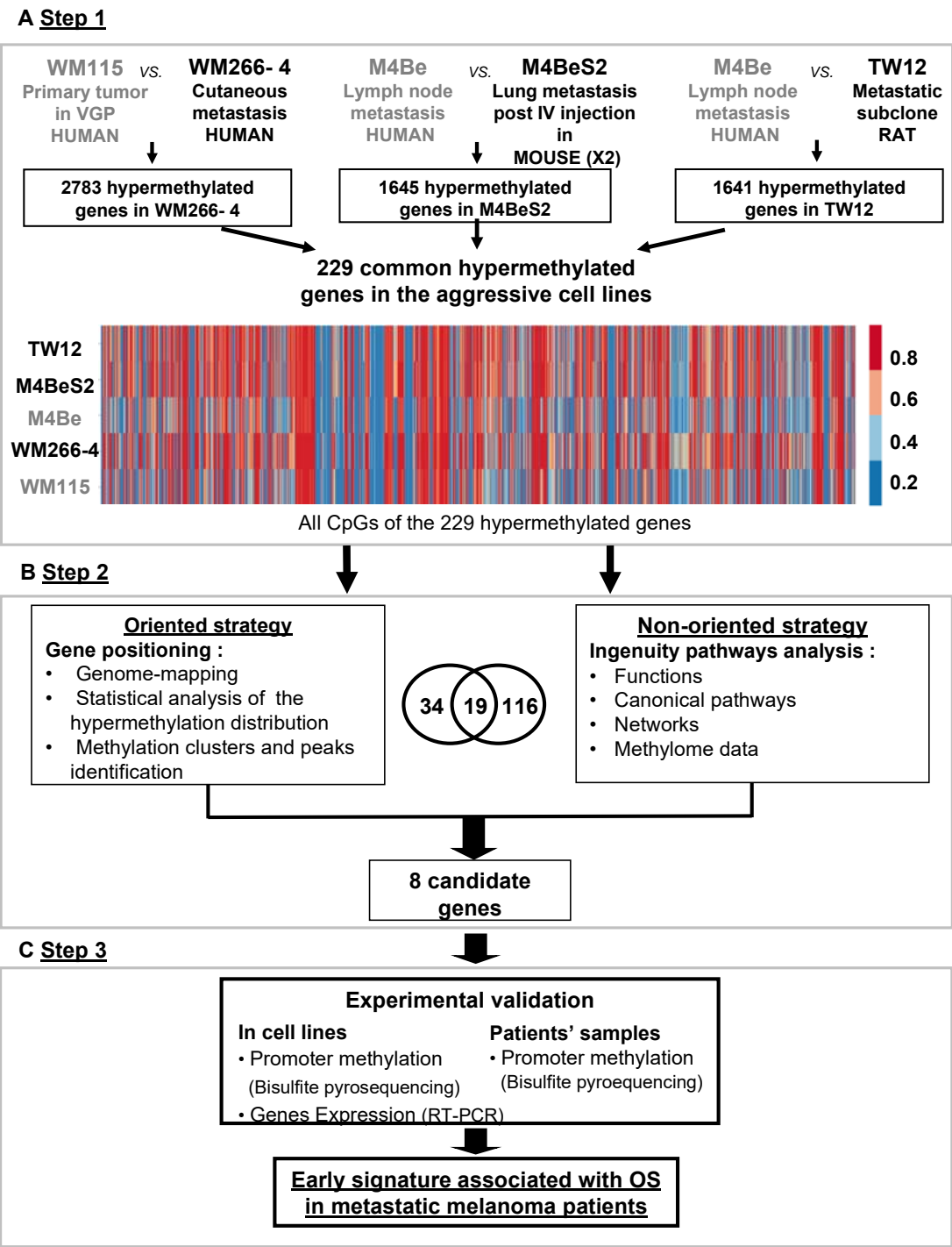


**Figure 1. Strategy for identifying differentially methylated genes signatures of aggressive melanoma.** The strategy is based on the analysis of three pairs of human melanoma cell lines with an aggressive variant derived under different physiological contexts: human, mouse and rat. In each pair, the cell line defined as more aggressive is indicated in bold characters. **A. Step1:** The methylation status of more than 480,000 CpG positions was compared in each cell line pair using the Illumina Infinium(®) Human Methylation 450K BeadChip technology. 229 common genes showing at least three CpGs positions with methylation levels increased by 20% in the aggressive cell line were retained (hypermethylated genes). **B. Step 2:** Two strategies for data analysis were used: the oriented

strategy is based on a statistical analysis of the distribution of the hypermethylated genes across the genome, and the non-oriented strategy uses Ingenuity Pathway Analysis (IPA) software to identify potential links to described networks and functions. **C. Step3:** Experimental validation of the selected genes, by bisulfite pyrosequencing for DNA methylation and RT-PCR for gene expression, was performed in the WM115 and WM266-4 cell lines prior to analysis in patient samples. After applying this differential threshold to at least three CpG positions for each gene we found that 2783, 1645, and 1641 genes were hypermethylated in WM266-4 vs. WM115, M4BeS2 vs. M4Be, and TW12 vs. M4Be, respectively (A). 229 genes, comprising 5590 CpG sites, were common to all three pairs of cell lines. These 229 genes were further analysed using the human WM115/WM266-4 pair. 1287 (23%) CpGs were hypermethylated (>20%) in WM266-4 cells, of which 788 (61%) were located in promoter regions (TSS1500-TSS200-5'UTR-1<sup>st</sup> exon), 452 (35%) in gene bodies and 47 (4%) in 3'UTR regions.

The DNA methylation profiles of each cell line was analysed using the Human Methylation 450K array BeadChip technology to identify the hypermethylated genes in the more aggressive variants. A first global analysis showed that nearly half of the analysed genes displayed at least one CpG position, where methylation levels are increased over 20% in the aggressive cell line compared to its respective counterpart. Following this first step of selection, we adopted two complementary approaches (Figure 1B). An oriented strategy, based on the genomic mapping of the 229 hypermethylated genes common to the aggressive melanoma cell lines, allowed us to identify clusters of hypermethylation. Clusters consisted of at least two hypermethylated genes that are either direct neighbours or separated within 3 megabases (Mb) of one another (Figure 2). Sex chromosomes were excluded from this analysis because they are subject to parental imprinting (20).

Bootstrap analysis of the repartition of the 229 genes along the chromosomes confirmed a non-random distribution, hypermethylated genes enriched in short chromosomal regions (Figure 2 and Supplementary Figure S1). Nine methylation clusters were identified on chromosomes 5, 6, 10, 15, 16, and 17 (dotted line circles in Figure 2 and list in Supplementary Table S1), containing a total of 74 genes (Supplementary Table S2). Among these genes, 34 were further selected because they displayed at least two hypermethylated CpGs located in the promoter region (TSS1500-TSS200-5'UTR-1<sup>ST</sup> exon) and a 40% difference in methylation when comparing human WM266-4 to WM115 cells. Chromosome 5 and 17 are of particular interest as the methylation clusters contain large multigenic families (Supplementary Figure S1). On chromosome 5, nine genes were identified as hypermethylated with a methylation cluster containing six genes belonging to the protocadherin beta (*PCDHB*) family (Supplementary Figure S1A and insert). *SPAG7*, *SOC3* and *RAC3* displayed the strongest hypermethylation values (over 90%) among the 10 hypermethylated genes found on chromosome 17, that had at least two CpGs in the promoter

region with a > 40% difference methylation in WM266-4 cells. Interestingly, this methylation cluster included five members of the multigenic Myosin heavy chain (MYH) family (insert in Supplementary Figure S1B).

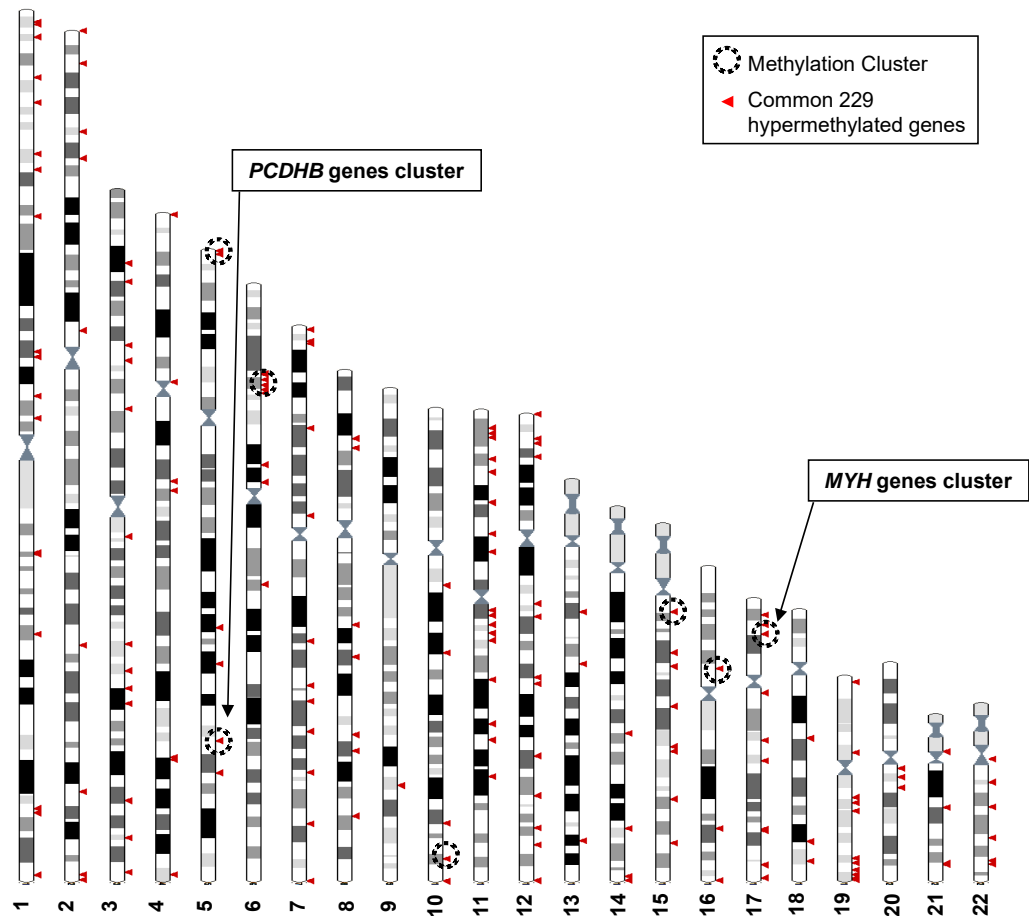


**Figure 2. Genomic distribution of the 229 commonly hypermethylated genes in the more aggressive cell lines.**

The Ensembl genome browser (<http://www.ensembl.org>, view on karyotype) was used to map the 229 hypermethylated genes to the human genome. Sex chromosomes were excluded from the analysis. Each arrowhead could correspond to several genes. Methylation clusters are indicated by dotted line circles. Chromosome 5 and 6 circles correspond to two clusters that are too close to be separated on this scale.

The second strategy was non-oriented and consisted of analysing the functional pathways in which the 229 hypermethylated genes were involved. Using QIAGEN Ingenuity® Pathway Analysis (IPA®, QIAGEN Redwood City, [www.qiagen.com/ingenuity](http://www.qiagen.com/ingenuity)) software, we found 116 genes highly associated with known functions ( $p < 0.05$ , Supplementary Table S3). The top functions, which might play a role in aggressiveness and carcinogenesis of the melanoma cells, were cell-to-cell signalling and interactions, cellular

assembly and organization, cancer and cellular movement. Finally, when cross-checking the 34 genes from the oriented strategy and the 116 genes from the non-oriented strategy, we identified 19 common genes (Figure 1B). Notably, all of 19 genes were associated with one or two of the top functional networks from the IPA (Supplementary Dataset1).

### **Gene selection and validation.**

The third part of our approach consisted of validating the methylation status of a subset of these candidate genes in melanoma cell lines and patient's tissues samples. Combining the cluster analysis and the IPA results, we chose in total eight genes distributed on four different chromosomes, bearing hypermethylation clusters, and selected for representing an hypermethylation peak, for showing a strong methylation difference between the aggressive and non-aggressive cell lines, and for the potential role in aggressiveness suggested by the literature (Supplementary Table S4). On chromosome 17, we chose the following four genes. **MYH1** was selected because it forms a highly differentially methylated cluster, (Supplementary Figure S1B) and is known to show aberrant expression levels in aggressive cells in head and neck squamous and lung carcinoma tumours (21). **SOCS3** and **RAC3** displayed among the highest hypermethylation peaks in our aggressive melanoma lines (92% and 96%, respectively), with a very high differential methylation score, above 70%, between WM266-4 and WM115 cells. In addition, **SOCS3** has previously been reported to be hypermethylated in melanoma (22), while loss of **RAC3** expression has been associated with impaired invasion in glioma and breast carcinoma cells (23,24). **HOXB2** was chosen for its lower methylation score (69%) and differential methylation score (45%). It has previously been associated with progression of bladder cancer when silenced by promoter hypermethylation, and it can be re-expressed upon demethylation treatment with 5-azacitidine (5azaC) (25). On chromosome 5, two genes were chosen from the PCDHB hypermethylation cluster: **PCDHB15** and **PCDHB16** that are CIMP-associated with bad prognosis in neuroblastoma (26,27). Of note, neurons and melanocytes originate from the same germ layer during embryogenesis. Furthermore, **BCL2L10** (B Cell Lymphoma 2 like 10) located on chromosome 15 was selected because it bears the highest methylation score (73%) on this chromosome, it is implicated in apoptosis, it was previously described as hypermethylated in gastric cancer cell lines (28), and associated with poor prognosis in gastric cancer patients (29,30). Finally, **MIR155HG**, located on chromosome 21, encodes a microRNA, miR-155, was chosen because linked to cell proliferation and cancer (31), including in melanoma where it is downregulated (32,33).

The methylation status of these eight genes (*MYH1*, *RAC3*, *SOCS3*, *HOXB2*, *PCDHB15*, *PCDHB16*, *BCL2L10*, *MIR155HG*) was further validated in WM115 vs WM266-4 cell lines by DNA pyrosequencing after bisulfite conversion and PCR amplification on 100 bp regions containing the CpGs identified in step 2 (Figure 1C). Seven genes pass the threshold of validation, 20% DNA methylation difference between the cell lines (Figure S2).

**Validation in patient samples and identification of a methylation signature.**

Next, we assessed the methylation profile of the eight selected genes in 20 tumour tissues from melanoma patients, of which 10 were from metastatic melanomas and 10 were from primary melanomas (Figure 1C). Four genes (*MYH1*, *PCDHB16*, *PCDHB15* and *BCL2L10*) showed a differential methylation profile between metastatic and primary tumour tissue samples (data not shown). For further validation, CpG sites in these four genes were individually analysed using bisulfite conversion followed by pyrosequencing in reference pair of cell lines (WM115/WM266-4) as well as two melanoma cell lines derived from the same patient: WM983A (primary site) and WM983B (lymph node metastatic site, Figure 3).

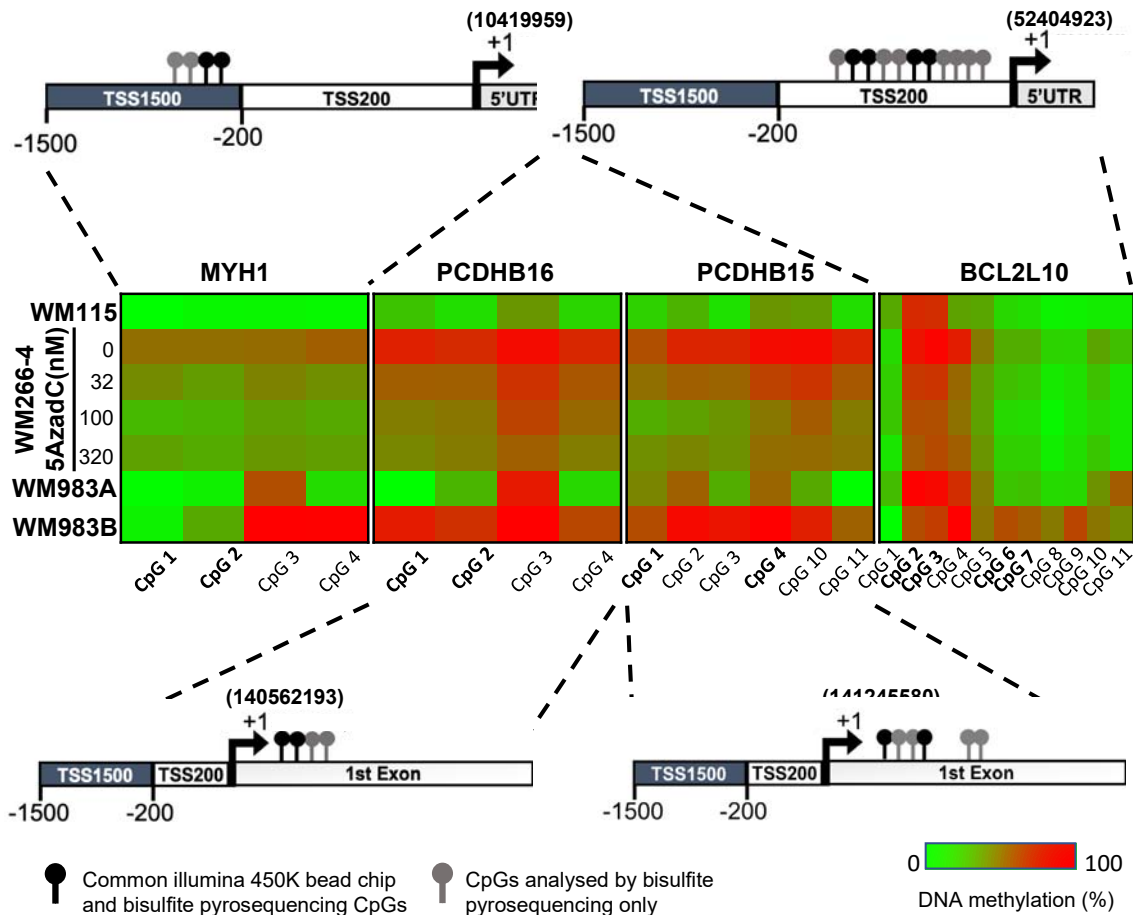


**Figure 3. Promoter hypermethylation of the candidate genes in cell lines.**

**A.** Shown is the localization of all the CpGs analysed (lollipops) on the four selected genes (*MYH1*, *PCDHB15*, *PCDHB16*, and *BCL2L10*). The CpGs present on the 450k array are in bold type (black lollipops). The heatmap indicates the DNA methylation percentage (red = 100, green = 0) of the indicated CpGs in each gene and each cell line. WM115 and WM983A are primary cell lines derived from two patients. WM266-4 and WM983B are the cutaneous and lymph node metastasis counterpart. WM266-4 cells were treated with daily doses of 5AzaC (32, 100, and 320 nM) 72 hours before genomic DNA extraction.

DNA methylation levels at each CpG site were analysed by bisulfite pyrosequencing, confirming a clear difference in methylation for the four genes in the aggressive tumour cells compared to less aggressive forms. Interestingly, this DNA methylation could be reversed in WM266-4 cells using a low dose of 5azadC treatment (32, 100, and 320nM). The median methylation of these individual CpGs was determined on the first set of patient samples, 10 metastatic and 10 primary tumours, and on additional 10 primary tumour samples (Supplementary Figure S3). Remarkably, the median of DNA methylation within primary samples appeared to be inversely correlated with patient overall survival (OS). Thus, we defined patients with primary tumours diagnosis and long survival (LS) with an OS >1 year and patients with short survival (SS) with an overall survival (OS, median survival = 6 months) ≤1 year (median survival = 51 months) after diagnosed. The DNA methylation profile in primary tumours with SS similar to that observed in metastatic patients (top, in red, Supplementary Figure S3). The analysis showed that *MYH1* was globally hypomethylated in SS patients, whereas *PCDHB16*, *PCDHB15*, and *BCL2L10* were hypermethylated. Data from 29 additional primary tumours samples were then analysed. The extended cohort of patient with primary melanoma primary (n=49) confirmed that these four differentially methylated genes represent specific markers of more aggressive SS primary and metastatic melanoma tumours (Figure 4A).



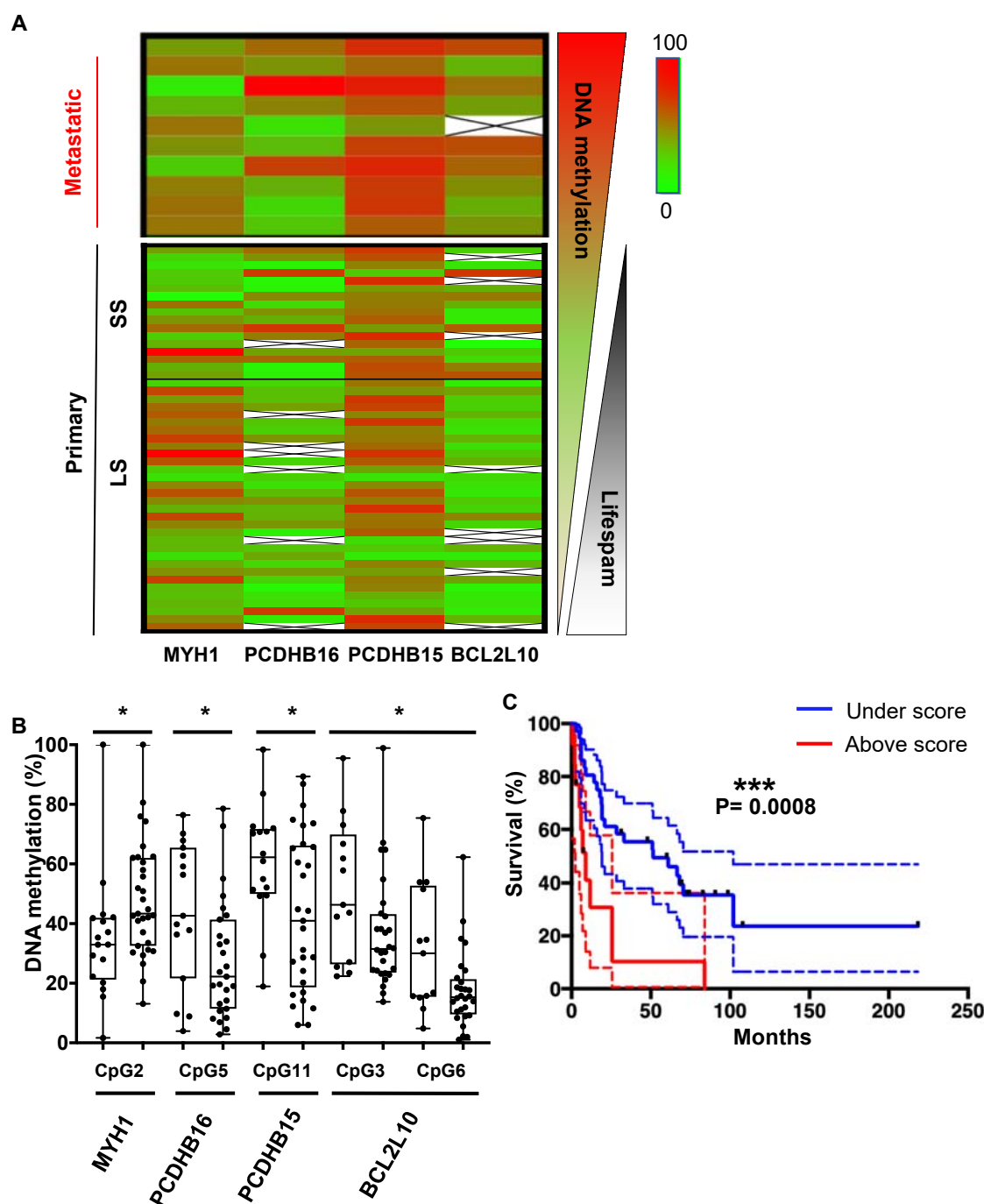


**Figure 4. CpGs DNA methylation in primary melanomas predicts patient outcome.**

**A.** The heatmap shows the median DNA methylation of analysed CpGs for each gene in metastatic (n=10) and primary (n=49) patient samples. Primary samples are divided by a black line indicating the cut-off at one year between the short and long survival (SS (left) and LS right)). **B.** DNA methylation changes in selected CpGs between short and long survival patients (n=49). Fisher test to analyse variances and t-Test were performed, \* = p < 0.05. **C.** Kaplan–Meier curve of patients’ survival based on the methylation score calculated for the five CpGs reported in panel B. The methylation score = 2 corresponds to at least two CpGs that showed a methylation difference >15% when compared to the DNA methylation median of the primary metastasis.

To determine the combination of CpGs that might predict melanoma aggressiveness, and thus survival outcome in patients with primary tumours, DNA methylation at individual CpG sites was analysed using bisulfite pyrosequencing (CpG positions are illustrated in Figure 3 and detailed in Supplementary Dataset2). One CpG showed significantly differential methylated in primary samples from SS patients (median SS = 6 months) when compared to LS patients (median LS = 51 months) for *PCDHB15*, *PCDBH16*, and *MYH1*, and two CpGs for *BCL2L10* (Figure 4B). DNA methylation *MYH1* CpG was inversely correlated with survival duration and was significantly hypomethylated in primary samples from SS patients; whereas *PCDHB16*, *PCDHB15*, and *BCL2L10* CpGs were hypermethylated in SS patients. To validate the robustness of this signature, a score was calculated as follows: a score of 1 was given to each gene when the median DNA methylation of the CpG met conditions for hypomethylation (>15%, seen for *MYH1*) and hypermethylation (>15%, for *PCDHB16*, *PCDHB15*, and *BCL2L10*). CpGs not meeting these criteria were given a score of 0. The final score was obtained by summing points attributed to each gene, so that scores range from 0 to 4 (Supplementary Dataset3). A threshold of 2 (*i.e.*, with at least two genes matching this condition) was used to include patients with a methylation score  $\geq 2$ . The methylation score was represented as a function of survival in months (Figure 4C and Supplementary Figure S4A). Patients with a methylation score  $\geq 2$  (red line) had a shorter life expectancy ( $\leq 1$  year) than those with a methylation score value  $< 2$  (blue line). This analysis demonstrated that a methylation score of at least 2 in primary melanoma samples is predictive of patient outcome (Log-rank test,  $p=0.0008$ ) with a significant Hazard Ratio of 3.4 ( $p = 0.001$ , concordance index = 0.62, Supplementary Figure S4B). Then, we compared the methylation score to the clinical parameter used in clinic, the Breslow index. Based on the melanoma AJCC staging (T1, T2, T3 and T4), we confirmed that on our 49 patient samples an increased Breslow depth of the primary tumour is a prognostic factor for survival probability (Kaplan-Meier plot in Supplementary Figure S4C). As our cohort contained only one sample of T1 grade (Primary tumour's depth less than 1mm), we then compared the survival probability between two groups: Breslow index below 2mm (T1 and T2) or above 2mm (T3 and T4). We obtained no statistical difference between the two groups (Supplementary Figures S4D and S4E), in contrast to what obtain upon use of the methylation signature (Supplementary Figures S4A and B). Most interestingly, the interaction between the methylation score and the Breslow index gave a significant increase of the hazard ratio from 3.4 to 6.3 ( $p < 0,001$ , concordance index = 0.63, Supplementary Figure S4F). This result support that the methylation score could improve the clinical prognostic utility of the Breslow index.

## DISCUSSION

To the best of our knowledge, the multistep strategy that we developed and used to identify differentially methylated genes in melanoma cells predicting aggressiveness is original. It is important to underline the starting point. We reasoned that, since epigenetic changes are linked to cell plasticity and biological environment changes (34–36), any common DNA methylation changes acquired by the most aggressive cells in different *in vivo* contexts (human, mouse and rat) would highlight a robust and relevant trait of melanoma tumour cell plasticity and aggressiveness despite their heterogeneity. Indeed, melanoma are highly heterogeneous tumours and until now it has been difficult to find a signature in primary melanoma, either based on DNA methylation or gene expression that help to predict prognosis as well as Breslow index (37). Several DNA methylation studies have been conducted comparing patient samples at different stages of cutaneous melanoma to normal samples, *i.e.*, melanocytes or nevi (38–41) or using cell lines derived from multi-grade patient samples (42) (9). While such studies have identified genes regulated by DNA methylation, none have yet identified a common pattern or a specific signature of melanoma aggressiveness. In contrast, the unique approach used in our study yielded a potential DNA methylation signature that correlates with outcomes.

Considering that the cellular models utilized, have experienced very different experimental microenvironments, we assumed that the common 229 identified hypermethylated genes represented genes either playing a direct role in or being associated with the aggressiveness of melanoma. Next, we applied a bootstrap analysis of the distribution of these hypermethylated genes revealing that they are not randomly distributed along the chromosomes, but are instead organized in clusters of hypermethylated genes. This observation of clustered genes regulated by DNA methylation is reminiscent of the mechanism underlying parental imprinting, and its spreading on imprinted genes during development (43,44). It is also coherent with the association of hypermethylated regions with long range epigenetic silencing (LRES) described by Frigola J. *et al* (45) in colon cancer, and with the fact that LRES regions containing hypermethylated genes extend up to 4 Mb and are correlated with gene extinction (46). Thus, guided by the hypothesis that these clustered genes correspond to early changes in CpG methylation during tumour progression, and may thus constitute a starting point for spreading of DNA methylation, we concentrated our efforts on these. An IPA analysis of the corresponding biological functions related to tumorigenesis or resistance to therapy, facilitated selection of eight potential genes that could be early signals of the aggressiveness

of the disease. The DNA methylation signature at these eight genes was analysed in additional melanoma cell lines (WM983A and WM983B) derived from the same patient, and in patient metastatic and primary tumour samples, highlighting four genes of interest. All four genes are demethylated upon treatment with 5AzadC in WM266-4 metastatic melanoma cells, and displayed the strongest methylation differential.

In the last part of our study, we challenged the methylation status of these four gene promoters in 59 patient samples. Surprisingly, five CpGs were significantly differentially methylated between patients with a short overall survival (<1-year, SS) and those with a longer overall survival (>1 year, LS). This led to the discovery of an early and robust signature of melanoma progression that is based directly on the primary tumour that can significantly predict patient outcome ( $p=0.0008$ ). Several studies have described different methylation patterns at various stages of melanoma disease, but only one reported a difference in methylation profile among primary tumour samples linking it to an ulceration status and thus a poor clinical outcome (47). More recently, Guo *et al.* (8) identified four DNA methylation biomarkers by analysing all melanoma types in the TCGA database, but without validating this on another patient cohort. Importantly, we have discovered CpG sites and genes that are key to metastatic melanoma formation and are grouped in genomic clusters. Our signature is unique, as is the integrated approach and the baseline assumption used to identify it. Going forward, a signature could be used to develop a much-needed early diagnostic DNA methylation kit, similar to existing kits for colon, lung and prostate cancer (48–50).

## CONCLUSIONS

We developed a novel multistep approach that allowed us to identify a methylation signature of five CpGs in primary melanoma tissues that has the potential to predict survival outcomes in cutaneous melanoma patients. Our method was based on two main concepts, the first one being that aggressive traits marked by DNA hypermethylation appear early in the disease and are independent of physiological context. The second concept is that hypermethylated sites in metastatic forms of melanoma are gathered in genomic clusters. On the methodological side, we combined analysis of the DNA methylome with chromosomal location. Following these general concepts, this integrated approach can be applied not only to other cancer types, but also to other diseases or biological processes such as aging and development.

## ABBREVIATIONS

5AzadC: 5aza-2'-deoxycytidine  
 AJCC: American joint committee on cancer  
 CIMP: CpG island methylator phenotype  
 CpG: Cytosine preceeding guanine nucleotide dimer 5'-3' direction  
 DNA: Deoxyribonucleic acid  
 FFPE: formalin-fixed paraffin-embedded  
 IPA: Ingenuity pathway analysis  
 LRES: Long range epigenetic silencing  
 LS: long survival  
 Mb: Megabases  
 OVS: overall survival  
 PCR: Polymerase chain reaction  
 RNA: ribonucleic acid  
 RRBS: Reduced representation bisulfite sequencing  
 SS: short survival  
 TCGA: The cancer genome atlas  
 TSS: Transcription start site  
 VGP: Vertical growth phase

## DATA AVAILABILITY

R-scripts are available upon request to the authors.  
 The DNA methylome dataset has been deposited in NCBI's Gene Expression Omnibus under the GEO Series accession number GSE155856  
<https://www.ncbi.nlm.nih.gov/geo/query/acc.cgi?acc=GSE155856>  
 The datasets supporting the conclusions of this article are included within the article and the following Supplementary files.

## SUPPLEMENTAL MATERIALS:

Supplementary file1.pdf: Supplementary figures and tables  
 Supplementary\_Dataset1.xls: IPA software networks results.  
 Supplementary\_Dataset2.xls: Bisulphite pyrosequencing primer, sequences, and CpG location.  
 Supplementary\_Dataset3.xlsx: Survival data and signature score for each patient sample.

573

## 574 **FUNDING**

575 This work was supported to P.B.A. by Centre National de la Recherche Scientifique (CNRS)  
576 [ATIP], Région Midi Pyrénées [Equipe d'Excellence and FEDER CNRS/Région Midi  
577 Pyrénées] and Fondation InNaBioSanté (project EpAM). It was carried out in the frame of the  
578 EU COST Action CM1406 Epigenetic Chemical Biology. D. Hoon and M. Bustos supported  
579 by Adelson Medical Research Foundation (AMRF USA).

580

## 581 **ACKNOWLEDGMENTS**

582 Not applicable.

583

## 584 **REFERENCES**

- 585 1. Moran B, Silva R, Perry AS, Gallagher WM. Epigenetics of malignant melanoma.  
586 *Semin Cancer Biol.* 2018;51:80–8.
- 587 2. Luke JJ, Flaherty KT, Ribas A, Long GV. Targeted agents and immunotherapies:  
588 optimizing outcomes in melanoma. *Nat Rev Clin Oncol.* 2017 Aug;14(8):463–82.
- 589 3. Teterycz P, Ługowska I, Koseła-Paterczyk H, Rutkowski P. Comparison of seventh and  
590 eighth edition of AJCC staging system in melanomas at locoregional stage. *World J Surg*  
591 *Oncol.* 2019 Jul 25;17(1):129.
- 592 4. Weiss SA, Wolchok JD, Sznol M. Immunotherapy of Melanoma: Facts and Hopes. *Clin*  
593 *Cancer Res Off J Am Assoc Cancer Res.* 2019 01;25(17):5191–201.
- 594 5. Tanemura A, Terando AM, Sim MS, van Hoesel AQ, de Maat MF, Morton DL, et al.  
595 CpG island methylator phenotype predicts progression of malignant melanoma. *Clin*  
596 *Cancer Res.* 2009 Mar 1;15(5):1801–7.
- 597 6. Micevic G, Theodosakis N, Bosenberg M. Aberrant DNA methylation in melanoma:  
598 biomarker and therapeutic opportunities. *Clin Epigenetics.* 2017;9:34.
- 599 7. de Unamuno Bustos B, Murria Estal R, Pérez Simó G, Simarro Farinos J, Pujol Marco  
600 C, Navarro Mira M, et al. Aberrant DNA methylation is associated with aggressive  
601 clinicopathological features and poor survival in cutaneous melanoma. *Br J Dermatol.*  
602 2018;179(2):394–404.
- 603 8. Guo W, Zhu L, Zhu R, Chen Q, Wang Q, Chen J-Q. A four-DNA methylation biomarker  
604 is a superior predictor of survival of patients with cutaneous melanoma. *eLife.* 2019 Jun  
605 6;8.
- 606 9. Chatterjee A, Stockwell PA, Ahn A, Rodger EJ, Leichter AL, Eccles MR. Genome-wide  
607 methylation sequencing of paired primary and metastatic cell lines identifies common  
608 DNA methylation changes and a role for EBF3 as a candidate epigenetic driver of  
609 melanoma metastasis. *Oncotarget.* 2017 Jan 24;8(4):6085–101.

10. Emran AA, Chatterjee A, Rodger EJ, Tiffen JC, Gallagher SJ, Eccles MR, et al. Targeting DNA Methylation and EZH2 Activity to Overcome Melanoma Resistance to Immunotherapy. *Trends Immunol.* 2019 Apr;40(4):328–44.
11. Michalak EM, Burr ML, Bannister AJ, Dawson MA. The roles of DNA, RNA and histone methylation in ageing and cancer. *Nat Rev Mol Cell Biol.* 2019;20(10):573–89.
12. Jacubovich R, Dor J-F. Tumour-associated antigens in culture medium of malignant melanoma cell strains. *Cancer Immunol Immunother* [Internet]. 1979 Oct [cited 2020 Jun 29];7(1). Available from: <http://link.springer.com/10.1007/BF00205410>
13. Bailly M, Doré JF. Human tumor spontaneous metastasis in immunosuppressed newborn rats. II. Multiple selections of human melanoma metastatic clones and variants. *Int J Cancer.* 1991 Nov 11;49(5):750–7.
14. Bertucci F, Pages C, Finetti P, Rochaix P, Lamant L, Devilard E, et al. Gene expression profiling of human melanoma cell lines with distinct metastatic potential identifies new progression markers. *Anticancer Res.* 2007 Oct;27(5A):3441–9.
15. Thomas CP, Buronfosse A, Portoukalian J, Fertil B. Correlation between the radiosensitivity in vitro of clones and variants derived from a human melanoma cell line and their spontaneous metastatic potential in vivo. *Cancer Lett.* 1995 Jan 27;88(2):221–5.
16. Clark EA, Golub TR, Lander ES, Hynes RO. Genomic analysis of metastasis reveals an essential role for RhoC. *Nature.* 2000 Aug 3;406(6795):532–5.
17. Gershenwald JE, Scolyer RA, Hess KR, Sondak VK, Long GV, Ross MI, et al. Melanoma staging: Evidence-based changes in the American Joint Committee on Cancer eighth edition cancer staging manual: Melanoma Staging: AJCC 8<sup>th</sup> Edition. *CA Cancer J Clin.* 2017 Nov;67(6):472–92.
18. Touleimat N, Tost J. Complete pipeline for Infinium((R)) Human Methylation 450K BeadChip data processing using subset quantile normalization for accurate DNA methylation estimation. *Epigenomics.* 2012 Jun;4(3):325–41.
19. Tost J, Gut IG. DNA methylation analysis by pyrosequencing. *Nat Protoc.* 2007;2(9):2265–75.
20. Barlow DP. Genomic imprinting: a mammalian epigenetic discovery model. *Annu Rev Genet.* 2011;45:379–403.
21. Vachani A, Nebozhyn M, Singhal S, Alila L, Wakeam E, Muschel R, et al. A 10-gene classifier for distinguishing head and neck squamous cell carcinoma and lung squamous cell carcinoma. *Clin Cancer Res Off J Am Assoc Cancer Res.* 2007 May 15;13(10):2905–15.
22. Tokita T, Maesawa C, Kimura T, Kotani K, Takahashi K, Akasaka T, et al. Methylation status of the SOCS3 gene in human malignant melanomas. *Int J Oncol.* 2007 Mar;30(3):689–94.

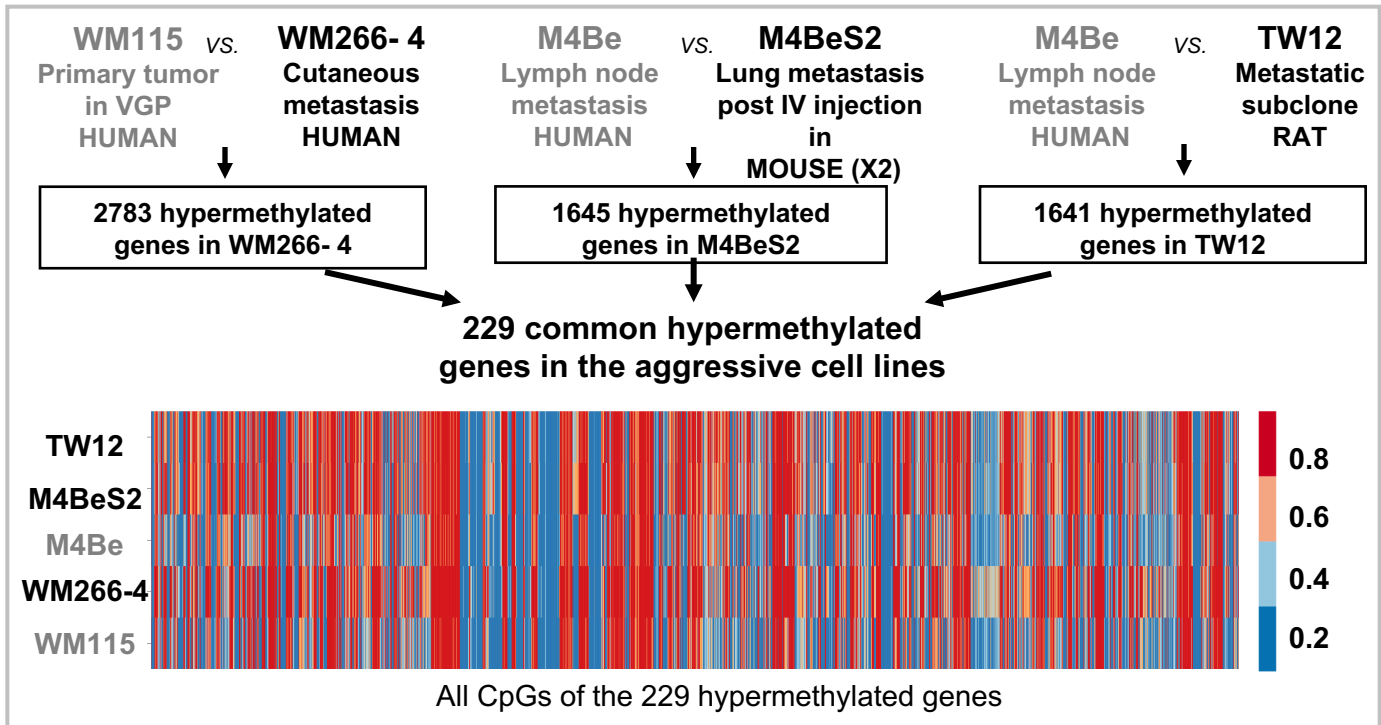


- 648 23. Chan AY, Coniglio SJ, Chuang Y, Michaelson D, Knaus UG, Philips MR, et al. Roles of  
649 the Rac1 and Rac3 GTPases in human tumor cell invasion. *Oncogene*. 2005 Nov  
650 24;24(53):7821–9.
- 651 24. Baugher PJ, Krishnamoorthy L, Price JE, Dharmawardhane SF. Rac1 and Rac3 isoform  
652 activation is involved in the invasive and metastatic phenotype of human breast cancer  
653 cells. *Breast Cancer Res BCR*. 2005;7(6):R965-974.
- 654 25. Marsit CJ, Houseman EA, Christensen BC, Gagne L, Wrensch MR, Nelson HH, et al.  
655 Identification of methylated genes associated with aggressive bladder cancer. *PLoS One*.  
656 2010;5(8):e12334.
- 657 26. Abe M, Ohira M, Kaneda A, Yagi Y, Yamamoto S, Kitano Y, et al. CpG island  
658 methylator phenotype is a strong determinant of poor prognosis in neuroblastomas.  
659 *Cancer Res*. 2005 Feb 1;65(3):828–34.
- 660 27. Banelli B, Brigati C, Di Vinci A, Casciano I, Forlani A, Borzi L, et al. A pyrosequencing  
661 assay for the quantitative methylation analysis of the PCDHB gene cluster, the major  
662 factor in neuroblastoma methylator phenotype. *Lab Invest*. 2012 Mar;92(3):458–65.
- 663 28. Mikata R, Fukai K, Imazeki F, Arai M, Fujiwara K, Yonemitsu Y, et al. BCL2L10 is  
664 frequently silenced by promoter hypermethylation in gastric cancer. *Oncol Rep*. 2010  
665 Jun;23(6):1701–8.
- 666 29. Xu JD, Cao XX, Long ZW, Liu XP, Furuya T, Xu JW, et al. BCL2L10 protein regulates  
667 apoptosis/proliferation through differential pathways in gastric cancer cells. *J Pathol*.  
668 2011 Feb;223(3):400–9.
- 669 30. Voso MT, Fabiani E, Piciocchi A, Matteucci C, Brandimarte L, Finelli C, et al. Role of  
670 BCL2L10 methylation and TET2 mutations in higher risk myelodysplastic syndromes  
671 treated with 5-azacytidine. *Leukemia*. 2011 Dec;25(12):1910–3.
- 672 31. Elton TS, Selemon H, Elton SM, Parinandi NL. Regulation of the MIR155 host gene in  
673 physiological and pathological processes. *Gene*. 2012 Dec 13;
- 674 32. Levati L, Alvino E, Pagani E, Arcelli D, Caporaso P, Bondanza S, et al. Altered  
675 expression of selected microRNAs in melanoma: antiproliferative and proapoptotic  
676 activity of miRNA-155. *Int J Oncol*. 2009 Aug;35(2):393–400.
- 677 33. Wang X, Bustos MA, Zhang X, Ramos RI, Tan C, Iida Y, et al. Downregulation of the  
678 Ubiquitin-E3 Ligase RNF123 Promotes Upregulation of the NF-κB1 Target SerpinE1 in  
679 Aggressive Glioblastoma Tumors. *Cancers*. 2020 Apr 27;12(5):E1081.
- 680 34. Hanahan D, Weinberg RA. Hallmarks of cancer: the next generation. *Cell*. 2011 Mar  
681 4;144(5):646–74.
- 682 35. Feinberg AP, Fallin MD. Epigenetics at the Crossroads of Genes and the Environment.  
683 *JAMA*. 2015 Sep 15;314(11):1129–30.
- 684 36. Feinberg AP, Ohlsson R, Henikoff S. The epigenetic progenitor origin of human cancer.  
685 *Nat Rev Genet*. 2006 Jan;7(1):21–33.

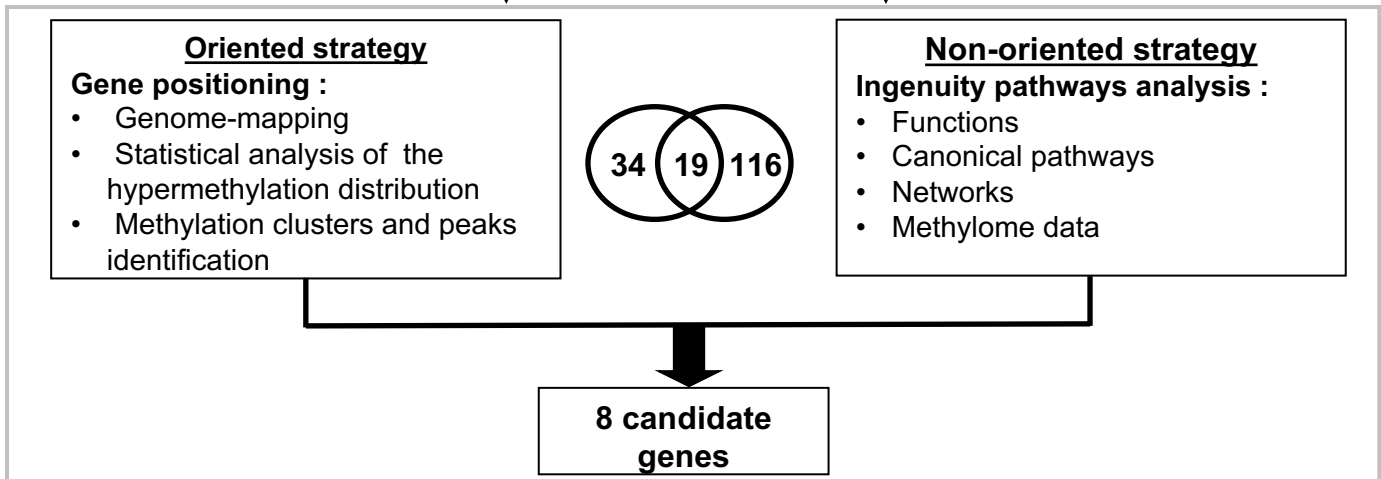
- 686 37. Bhalla S, Kaur H, Dhall A, Raghava GPS. Prediction and Analysis of Skin Cancer  
687 Progression using Genomics Profiles of Patients. *Sci Rep*. 2019 Oct 31;9(1):15790.
- 688 38. Marzese DM, Scolyer RA, Huynh JL, Huang SK, Hirose H, Chong KK, et al.  
689 Epigenome-wide DNA methylation landscape of melanoma progression to brain  
690 metastasis reveals aberrations on homeobox D cluster associated with prognosis. *Hum*  
691 *Mol Genet*. 2014 Jan 1;23(1):226–38.
- 692 39. Gao L, Smit MA, van den Oord JJ, Goeman JJ, Verdegaal EM, van der Burg SH, et al.  
693 Genome-wide promoter methylation analysis identifies epigenetic silencing of MAPK13  
694 in primary cutaneous melanoma. *Pigment Cell Melanoma Res*. 2013 Jul;26(4):542–54.
- 695 40. Sigalotti L, Covre A, Fratta E, Parisi G, Sonogo P, Colizzi F, et al. Whole genome  
696 methylation profiles as independent markers of survival in stage iiii melanoma patients.  
697 *J Transl Med*. 2012 Sep 5;10(1):185.
- 698 41. Marzese DM, Witz IP, Kelly DF, Hoon DSB. Epigenomic landscape of melanoma  
699 progression to brain metastasis: unexplored therapeutic alternatives. *Epigenomics*.  
700 2015;7(8):1303–11.
- 701 42. Li JL, Mazar J, Zhong C, Faulkner GJ, Govindarajan SS, Zhang Z, et al. Genome-wide  
702 methylated CpG island profiles of melanoma cells reveal a melanoma coregulation  
703 network. *Sci Rep*. 2013;3:2962.
- 704 43. Lewis A, Reik W. How imprinting centres work. *Cytogenet Genome Res*. 2006;113(1–  
705 4):81–9.
- 706 44. Lindsay H, Adams RL. Spreading of methylation along DNA. *Biochem J*. 1996 Dec  
707 1;320 ( Pt 2):473–8.
- 708 45. Frigola J, Song J, Stirzaker C, Hinshelwood RA, Peinado MA, Clark SJ. Epigenetic  
709 remodeling in colorectal cancer results in coordinate gene suppression across an entire  
710 chromosome band. *Nat Genet*. 2006 May;38(5):540–9.
- 711 46. Coolen MW, Stirzaker C, Song JZ, Statham AL, Kassir Z, Moreno CS, et al.  
712 Consolidation of the cancer genome into domains of repressive chromatin by long-range  
713 epigenetic silencing (LRES) reduces transcriptional plasticity. *Nat Cell Biol*. 2010  
714 Mar;12(3):235–46.
- 715 47. Rakosy Z, Ecsedi S, Toth R, Vizkeleti L, Hernandez-Vargas H, Hernandez-Vargas H, et  
716 al. Integrative genomics identifies gene signature associated with melanoma ulceration.  
717 *PloS One*. 2013;8(1):e54958.
- 718 48. Payne SR. From discovery to the clinic: the novel DNA methylation biomarker  
719 (m)SEPT9 for the detection of colorectal cancer in blood. *Epigenomics*. 2010  
720 Aug;2(4):575–85.
- 721 49. Kneip C, Schmidt B, Seegebarth A, Weickmann S, Fleischhacker M, Liebenberg V, et  
722 al. SHOX2 DNA methylation is a biomarker for the diagnosis of lung cancer in plasma.  
723 *J Thorac Oncol Off Publ Int Assoc Study Lung Cancer*. 2011 Oct;6(10):1632–8.

- 724 50. Li Y-W, Kong F-M, Zhou J-P, Dong M. Aberrant promoter methylation of the vimentin  
725 gene may contribute to colorectal carcinogenesis: a meta-analysis. Tumour Biol J Int  
726 Soc Oncodevelopmental Biol Med. 2014 Jul;35(7):6783–90.

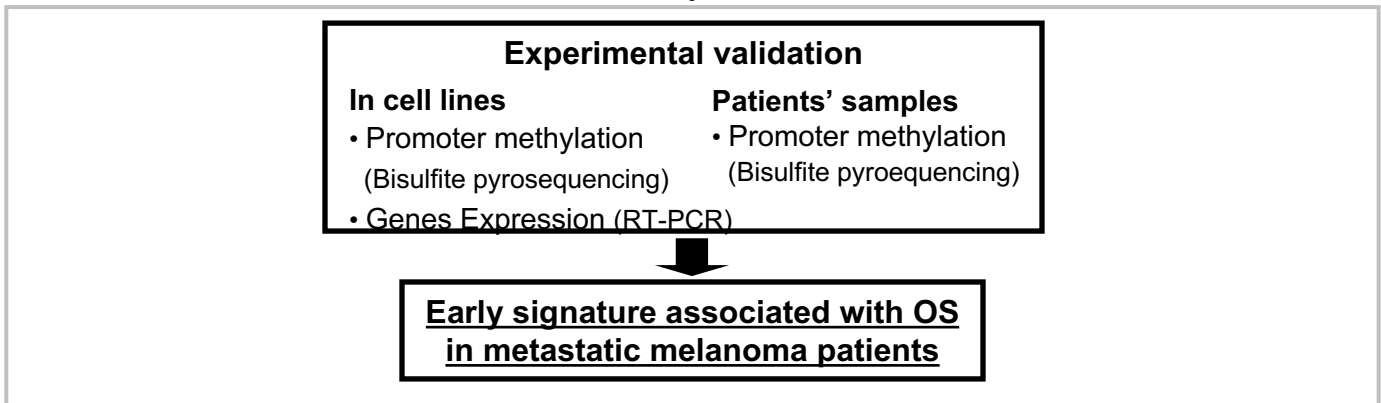
## A Step 1

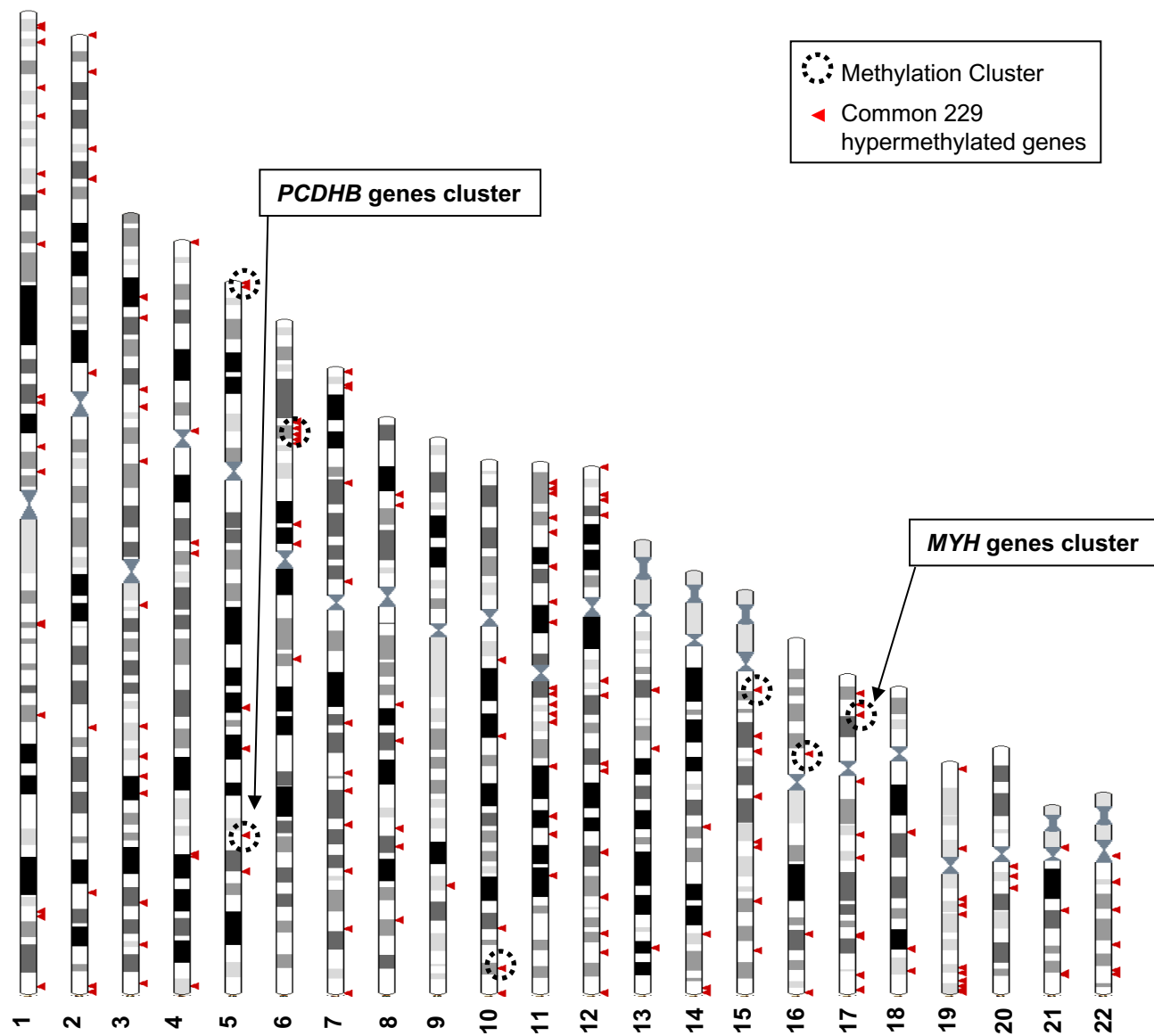


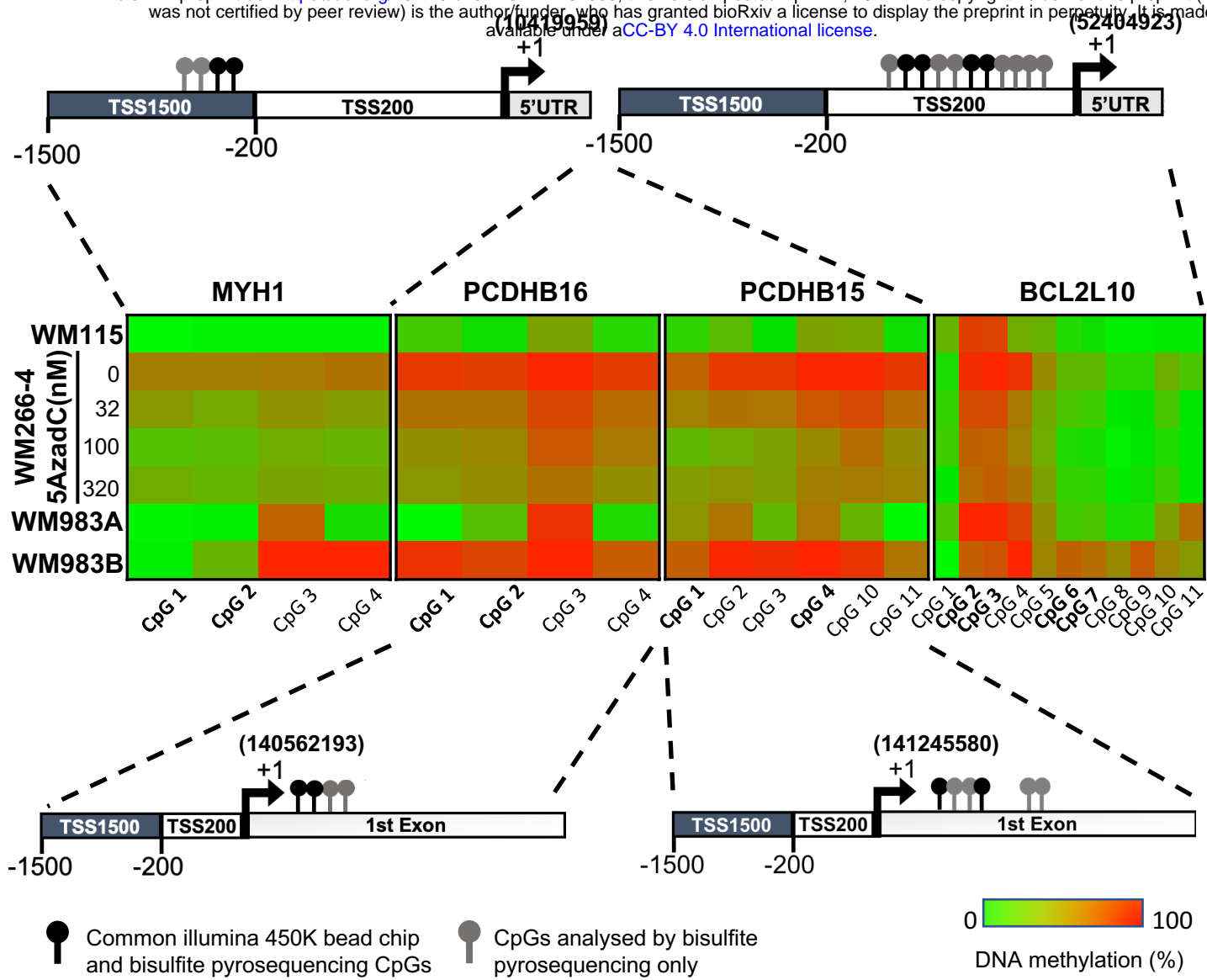
## B Step 2



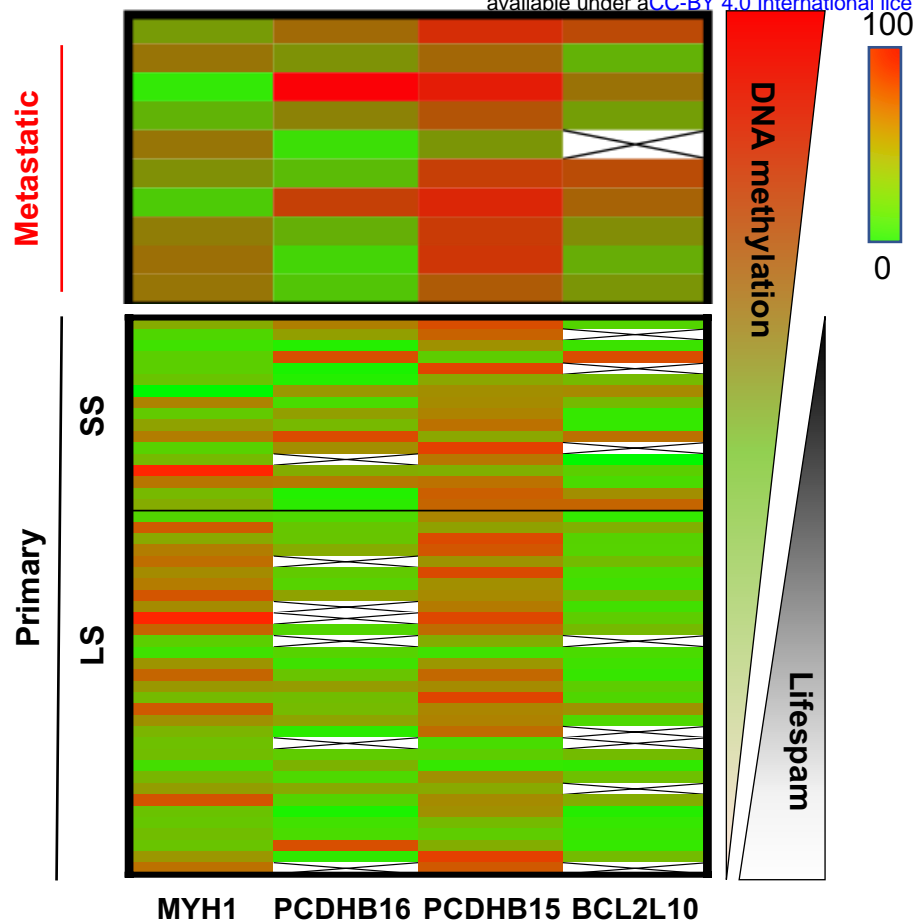
## C Step 3



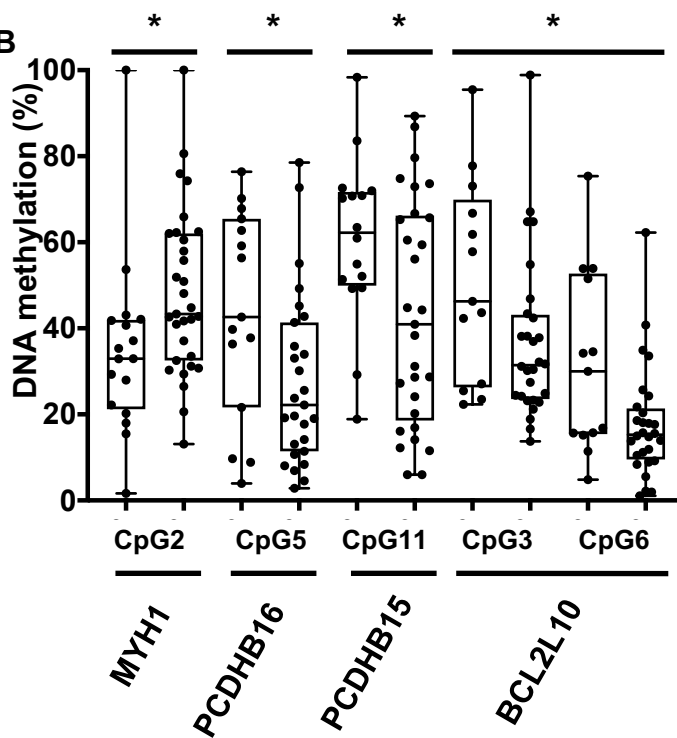




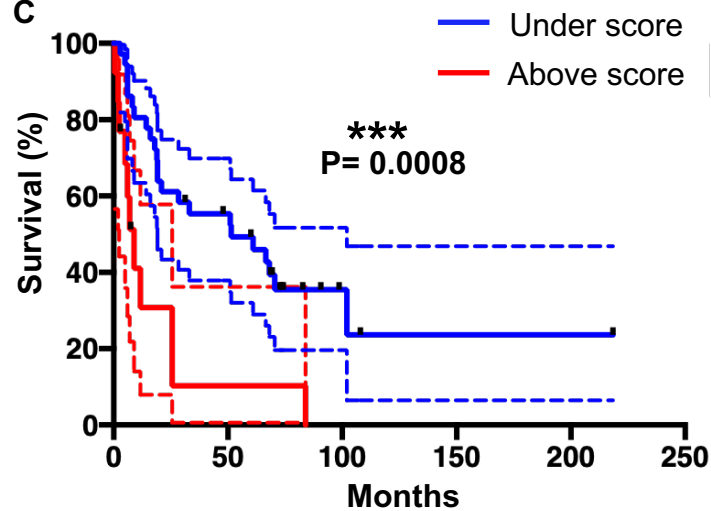
**A**



**B**



**C**





## **Supplementary Information for**

DNA methylome combined with chromosome cluster-oriented analysis provides an early signature for cutaneous melanoma aggressiveness.

Arnaud Carrier, Cécile Desjobert, Loïc Ponger, Laurence Lamant, Matias Bustos, Jorge Torres-Ferreira, Rui Henrique, Carmen Jeronimo, Luisa Lanfranccone, Audrey Delmas, Gilles Favre, Antoine Daunay, Florence Busato, Dave S.B. Hoon, Jörg Tost, Chantal Etievant, Joëlle Riond, Paola B. Arimondo\*

Corresponding author Paola B. Arimondo  
Email: [paola.arimondo@cncrs.fr](mailto:paola.arimondo@cncrs.fr)

### **This PDF file includes:**

Figures S1 to S4  
Table S1 to S5

### **Other supplementary materials for this manuscript include the following:**

Datasets S1 to S3

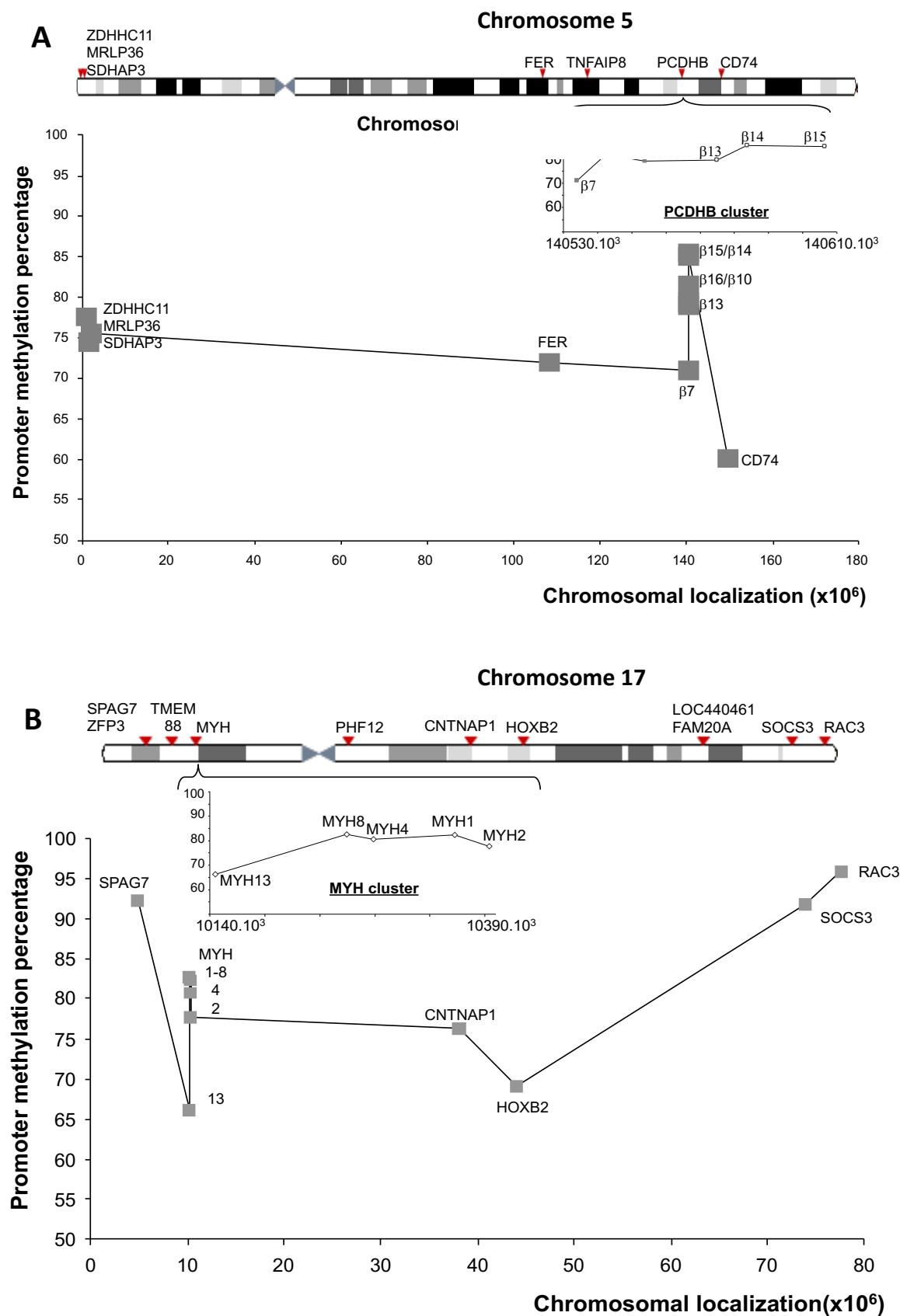


**Fig. S1.** Examples of genomic localization of the genes hypermethylated in the most aggressive cell lines. Promoter methylation scores correspond to the average methylation values at CpG positions located in the promoter regions showing an increased methylation above 20% in WM266-4 compared to WM115 cells. The genes are indicated on the “band giemsa-related” representation (arrows). The graph shows genes with at least two CpGs in the promoter region with DNA methylation differences over 40% between WM266-4 and WM115 cells (grey squares).

- A) Localization and promoter methylation score of nine hypermethylated genes found on chromosome 5. The PCDH $\beta$  genes cluster is magnified in the insert.
- B) Localization and promoter methylation score of 15 hypermethylated genes found on chromosome 17; five of them belong to the MYH1 cluster (insert).

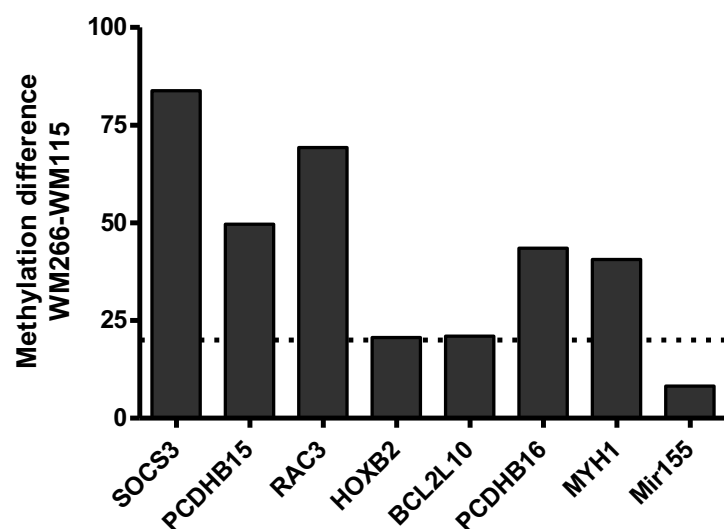


**Fig. S2. Promoter hypermethylation of the candidate genes in WM266-4 vs WM115 cells.**  
Hypermethylation (Methylation difference  $\geq 20\%$ : dotted line) for all candidate genes analysed by Bisulfite-Pyrosequencing.

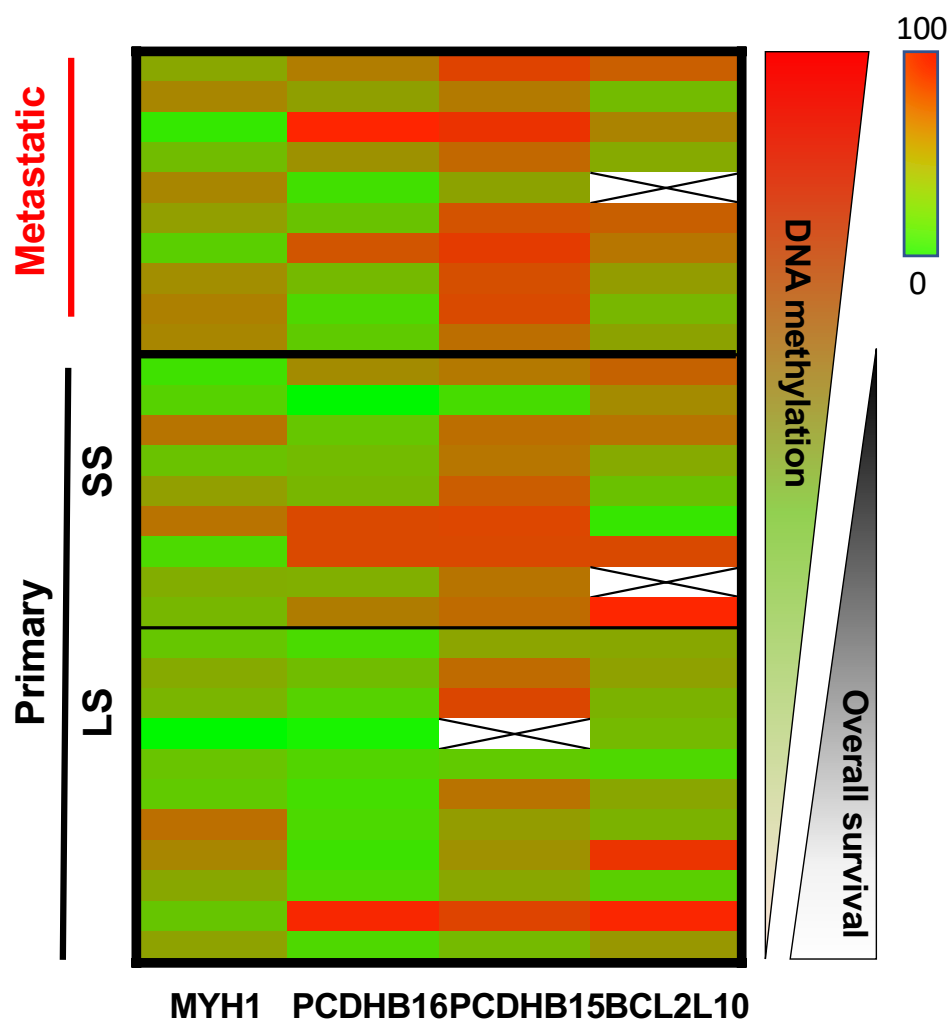


**Fig. S3. Heatmap of DNA methylation of MYH1, PCDHB16, PCDHB15 and BCL2L10 in the first set of 10 metastatic melanoma patient sample and 20 primary patient melanoma.**

The median DNA methylation of the analysed CpG for each gene is indicated as percentage and overall survival in months. Primary samples are divided by a small black line indicating the cut-off at one year between the short and long overall survival (SS and LS).

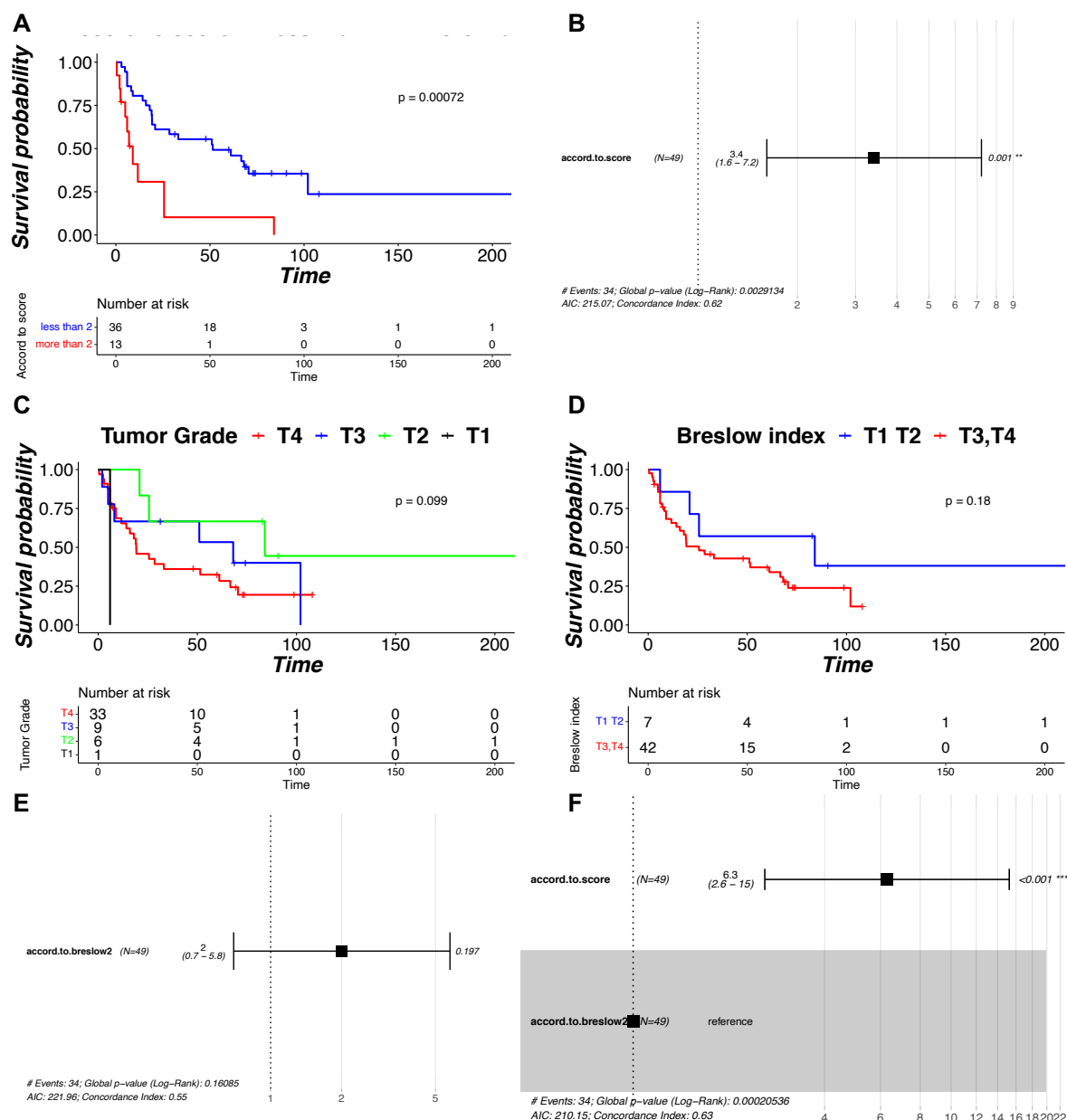


**Fig. S4. The DNA methylation score is a better prognostic factor than classical used clinical parameter Breslow index.**

- Kaplan-Meier curve of patients based on the methylation score in the 49 primary melanoma samples.
- Hazard ratio plot calculated from our methylation score on the 49 primary melanoma samples.
- Kaplan-Meier curve of patients according to the primary tumor grade defined by the AJCC staging system of melanoma from Breslow index (Primary tumor T1 = less than 1mm, T2 = less than 2 mm, T3 = between 2 and 4 mm, T4 = more than 4 mm).
- Kaplan-Meier curve of patients based on the Breslow index in the 49 primary melanoma samples (less than 2 in blue: T1 and T2 grade, more than 2 in red: T3 and T4 grades).
- Hazard ratio plot calculated from Breslow index on the 49 primary melanoma samples.
- Hazard ratio plot calculated from the interaction between our methylation score and the Breslow index on the 49 primary melanoma samples.

**Table S1 - Clusters of hypermethylated genes identified by the oriented strategy.**

Nine methylation clusters containing 29 genes on six chromosomes.


















Cluster	Gene Name	Ensembl Gene ID	EntrezGene ID	chromosome	Ref Seq Genes Position	
					Start (bp)	end (bp)
1	SDHAP3	ENSG00000185986	728609	5	1572073	1594646
	MRPL36	ENSG00000171421	64979	5	1798499	1799956
2	PCDHB16	ENSG00000196963	57717	5	140561265	140565796
	PCDHB9	ENSG00000120324	56127	5	140566893	140571111
3	PCDHB13	ENSG00000187372	56123	5	140593491	140596993
	PCDHB14	ENSG00000120327	56122	5	140601898	140605860
	PCDHB18	ENSG00000146001	54660	5	140613938	140617101
	PCDHB15	ENSG00000113248	56121	5	140624917	140627801
4	KIAA1949/PPP1R18	ENSG00000146112	170954	6	30644166	30655672
	NRM	ENSG00000137404	11270	6	30655824	30659197
	MDC1	ENSG00000137337	9656	6	30667584	30685458
5	BAT4/GPANK1	ENSG00000204438	7918	6	31629006	31633407
	CSNK2B	ENSG00000204435	1460	6	31633657	31637843
6	DOCK1	ENSG00000150760	1793	10	128594023	129250780
	FAM196A	ENSG00000188916	642938	10	128933690	128994422
7	SNORD115-15	ENSG00000201679	100033453	15	25451409	25477615
	SNORD115-21	ENSG00000199833	100033603	15	25453230	25453310
	SNORD115-42	ENSG00000201143	100033816	15	25492492	25492573
8	BOLA2	ENSG00000183336	552900	16	29464914	29466285
	BOLA2B	ENSG00000169627	654483	16	29464914	29466285
	GIYD1/SLX1A	ENSG00000132207	548593	16	29465822	29469545
	GIYD2	ENSG00000181625	79008	16	29465822	29469545
	SULT1A3	ENSG00000261052	6818	16	29471207	29476301
	SULT1A4	ENSG00000213648	445329	16	29471207	29476301
9	MYH13	ENSG00000006788	8735	17	10204183	10276322
	MYH8	ENSG00000133020	4626	17	10293642	10325267
	MYH4	ENSG00000264424	4622	17	10346608	10372876
	MYH1	ENSG00000109061	4619	17	10395627	10421859
	MYH2	ENSG00000125414	4620	17	10424465	10453017



**Table S2: List of the 74 hypermethylated genes found on six chromosomes bearing at least one cluster.**

Gene name	Ensembl gene ID	Chromosome
CD74	ENSG00000019582	5
FER	ENSG000000151422	5
MRPL36	ENSG000000171421	5
NKD2	ENSG000000145506	5
PCDHB10	ENSG000000120324	5
PCDHB13	ENSG000000187372	5
PCDHB14	ENSG000000120327	5
PCDHB15	ENSG000000113248	5
PCDHB16	ENSG000000196963	5
PCDHB18	ENSG000000146001	5
PCDHB7	ENSG000000113212	5
PCDHB9	ENSG000000120324	5
SDHAP3	ENSG000000185986	5
TNFAIP8	ENSG000000145779	5
ZDHHC11	ENSG000000188818	5
BAG2	ENSG000000112208	6
BAT4	ENSG000000204438	6
CSNK2B	ENSG000000204435	6
HIST1H3I	ENSG000000182572	6
HSPA1L	ENSG000000204390	6
IL17A	ENSG000000112115	6
KIAA1949	ENSG000000146112	6
MDC1	ENSG000000137337	6
NRM	ENSG000000137404	6
NT5E	ENSG000000135318	6
OR12D2	ENSG000000168787	6
PRR3	ENSG000000204576	6
RGL2	ENSG000000237441	6
TCF19	ENSG000000137310	6
TRIM26	ENSG000000234127	6
ZNF389	ENSG000000226314	6
C10orf53;C10orf53	ENSG000000178645	10
CYP2E1	ENSG000000130649	10
DNA2	ENSG000000138346	10
DOCK1	ENSG000000150760	10
FAM196A	ENSG000000188916	10
KIAA1598	ENSG000000187164	10
ANKDD1A	ENSG000000166839	15
BCL2L10	ENSG000000137875	15
C15orf2	ENSG000000185823	15
CHRNA3	ENSG000000080644	15
CSNK1A1P	ENSG000000223518	15
FBXL22	ENSG000000197361	15
GCHFR	ENSG000000137880	15
PIF1	ENSG000000140451	15
RCCD1	ENSG000000166965	15
SNORD115-15	ENSG000000201679	15
SNORD115-21	ENSG000000199833	15
SNORD115-42	ENSG000000201143	15
BOLA2	ENSG000000183336	16
BOLA2B	ENSG000000169627	16
GIYD1	ENSG000000132207	16
GIYD2	ENSG000000181625	16
SPIRE2	ENSG000000204991	16
SULT1A3	ENSG000000261052	16
SULT1A4	ENSG000000213648	16
ZNRF1	ENSG000000186187	16
CNTNAP1	ENSG000000108797	17
FAM20A	ENSG000000108950	17
FASN	ENSG000000169710	17
HOXB2	ENSG000000173917	17
HOXB6	ENSG000000108511	17
LOC440461	ENSG000000267472	17
MYH1	ENSG000000109061	17
MYH13	ENSG00000006788	17
MYH2	ENSG000000125414	17
MYH4	ENSG000000264424	17
MYH8	ENSG000000133020	17
PHF12	ENSG000000109118	17
RAC3	ENSG000000169750	17
SOC3	ENSG000000184557	17
SPAG7	ENSG000000091640	17
TMEM88	ENSG000000167874	17
ZFP3	ENSG000000180787	17

**Table S3: Top Functions associated by IPA to the 229 hypermethylated genes in the aggressive cell lines.** Among the 229 genes, 116 were associated to IPA canonical functions. Column 1 indicates the top functions. Column 2 shows the  $-\log(p\text{-value})$  as horizontal histogram relative to the Fisher exact test ( $p < 0.05$  :  $-\log(0.05) = 1.3$  =threshold) used by IPA to classify the most representative functions. The score in column 3 corresponds to the number of genes among the 229 belonging to the associated function.

Functions	$-\log(p\text{-value})$	Score
Cell-to-cell signaling and interaction		27
Cellular assembly and organization		40
Cellular function and maintenance		41
Nervous system development and function		29
Tissue development		42
Cancer		62
Skeletal and muscular disorders		18
Tissue morphology		30
Gastrointestinal disease		50
Endocrine system disorders		26
Hepatic system disease		22
Metabolic disease		23
Cell morphology		27
Cellular development		30
Lipid metabolism		20
Small molecule biochemistry		34
Cellular movement		38

**Table S4: Detailed informations of the eight selected genes.**

Gene symbol	Gene	RefSeqGene	Chromosome	Methylation location	$\Delta$ methylation (%) ( $\beta$ WM266-4 - $\beta$ WM115) x 100	WM266-4 cells promotor methylation (%)	IPA Function
MYH1	myosin, heavy chain 1	NM_005963	17	cluster	75	82	Cellular assembly and organization, cancer
SOCS3	suppressor of cytokine signaling 3	NM_003955		Methylation peak	72	92	Cancer
RAC3	RAS-related C3 botulinum toxin substrate 3	NM_005052		Methylation peak	70	96	Cellular assembly and organization, cancer, cellular movement
HOXB2	homeobox B2	NM_002145		chromosome	45	69	Tissue development
PCDHB15	protocadherin beta 15	NM_018935	5	cluster	45	85	cell-to-cell signaling and interaction
PCDHB16	protocadherin beta 16	NM_020957		cluster	52	82	cell-to-cell signaling and interaction
BCL2L10	BCL2-like 10	NM_020396	15	chromosome	46	73	Cancer
Mir-155HG	Mir-155 Host Gene	NR_001458	21	other	32	74	Cancer

**Table S5 - Primers informations for RT-PCR and RT-qPCR experiments.**

Name	Primer	Amplicon size (bp)	Primer size	Tm (°C)	Sequence 5'-3'
PCDHB15	forward	101	20	56	TTGTAGCCAACCTGGCCAAT
	Reverse	101	20	57	AAGCTGCAAGCCTTGTTTCGT
SOCS3	forward	214	20	59	CAAGGACGGAGACTTCGATT
	Reverse	214	20	60	GCTGGTACTCGCTCTTGGAG
PCDHB16	forward	172	20	60	TATGAAGTGCGCATCAAAGC
	Reverse	172	20	60	TGCTGTTTTTCAGCGTTTCAG
HOXB2	forward	237	20	59	TTTAGCCGTTTCGCTTAGAGG
	Reverse	237	20	59	CCTTTTTCCGAGGAAGAGCT
BCL2L10	Forward	252	22	60	CCTTCATTTATCTCTGGACACG
	Reverse	252	19	60	TTTCACTCAAGGAAGAGCC
RAC3	Forward	109	20	60	GACAAGGACACCATTGAGCG
	Reverse	109	23	59	AGCACTCCAGGTATTTACAGAG
TBP	Forward	67	26	60	TTGACCTAAAGACCATTGCACTTCGT
	Reverse	67	20	60	TTACCGCAGCAAACCGCTTG
MYH1	RT <sup>2</sup> qPCR Primer assay (Qiagen)	136		60	330001 PPH14690E
MIR155HG	hsa-mir-155		21	60	CUGUUAUAGCUAAUCGUGAUA

**Dataset S1** - Results from the IPA software networks.

**Dataset S2** – Gene sequences, Illumina CpGs and bisulfite pyrosequencing primers

**Dataset S3** – Survival data and signature score for each patient sample.